



OPEN ACCESS

EDITED BY

Davide Tiranti,
Agenzia Regionale per la Protezione
Ambientale del Piemonte (Arpa
Piemonte), Italy

REVIEWED BY

Dario Gioia,
National Research Council (CNR), Italy
Giuseppe Corrado,
University of Basilicata, Italy

*CORRESPONDENCE

Vincenzo De Santis,
✉ vincenzo.desantis@uniba.it

RECEIVED 15 August 2023

ACCEPTED 21 September 2023

PUBLISHED 12 October 2023

CITATION

De Santis V, Scicchitano G, Scardino G,
Mele D, Sulpizio R, Colangelo G,
Zingaro M, Antonino NL, Tomaselli V and
Caldara M (2023), Construction of a
deltaic strandplain during the Roman
period in the Tavoliere di Puglia plain and
palaeoclimatic implications.
Front. Earth Sci. 11:1278105.
doi: 10.3389/feart.2023.1278105

COPYRIGHT

© 2023 De Santis, Scicchitano, Scardino,
Mele, Sulpizio, Colangelo, Zingaro,
Antonino, Tomaselli and Caldara. This is
an open-access article distributed under
the terms of the [Creative Commons
Attribution License \(CC BY\)](https://creativecommons.org/licenses/by/4.0/). The use,
distribution or reproduction in other
forums is permitted, provided the original
author(s) and the copyright owner(s) are
credited and that the original publication
in this journal is cited, in accordance with
accepted academic practice. No use,
distribution or reproduction is permitted
which does not comply with these terms.

Construction of a deltaic strandplain during the Roman period in the Tavoliere di Puglia plain and palaeoclimatic implications

Vincenzo De Santis^{1*}, Giovanni Scicchitano¹, Giovanni Scardino¹, Daniela Mele¹, Roberto Sulpizio¹, Giuseppe Colangelo², Marina Zingaro¹, Natasha Luigia Antonino³, Valeria Tomaselli⁴ and Massimo Caldara¹

¹Department of Earth and Geoenvironmental Sciences, University of Bari "Aldo Moro", Bari, Italy, ²Freelance Environmental and Forestry Sciences, Bari, Italy, ³Department of Humanities Research and Innovation, University of Bari "Aldo Moro", Bari, Italy, ⁴Department of Biosciences, Biotechnology and the Environment University of Bari "Aldo Moro", Bari, Italy

In response to the accidental exhumation of three ancient trees by farmers, we conducted a multidisciplinary study based on the stratigraphic analysis of boreholes, carbon-14 dating, aerial photo interpretation, and analysis of palaeobotanical and archaeological evidences. We reconstructed the formation and evolution during Roman times of a first "continuous" and then "discontinuous" deltaic strandplain at the mouth of the Carapelle Stream in the Tavoliere di Puglia Plain—the second-largest plain in Italy. Two main phases can be recognised in the evolution of the Carapelle deltaic strandplain: 1) a first phase, lasted until ca. the birth of Christ, was characterised by a regular and continuous construction of sand ridges one leaning against the other; 2) a second phase, lasted more or less from the birth of Christ to the termination of the construction of the deltaic strandplain, was characterised by the discontinuous construction of sand ridges/coastal barriers with the isolation of lagoons/ponds, and by evidences of alluvial events. The most probable climatic–environmental scenario to have formed the Roman-period deltaic strandplain implied that: 1) the first phase was triggered by a higher total amount of precipitations, but with less extreme alluvial events; 2) the second phase was triggered by a total amount of precipitation lower than the previous period, but with higher occurrence of extreme alluvial events and/or by extreme alluvial events separated by longer period of low precipitations. This second phase was enhanced by the opening of vegetation. The passage between the first and second phase of the Carapelle deltaic strandplain coincides with the passage from overall negative NAO index to an overall positive NAO index.

KEYWORDS

deltaic strandplain, Holocene, Roman tree trunks, palaeoclimate, multidisciplinary

1 Introduction

The Holocene, despite its brevity, has been characterised by many short-term natural climatic events (O'Brien et al., 1995; Bond et al., 1997; Bond et al., 2001; Mayewski et al., 2004; Wanner et al., 2011; De Santis and Caldara, 2015). These events have driven the geomorphological dynamics of recently formed landscapes, including the Holocene coastal alluvial plains.

These short-term pulses manifested as abrupt changes in Europe and other parts of the Northern Hemisphere (O'Brien et al., 1995; Ljungqvist, 2010; Wanner et al., 2011). Bond et al. (1997, 2001), Bradley et al. (2003), Mayewski et al. (2004), Ljungqvist (2010), Wanner et al. (2011), and others identified these Northern Hemisphere Holocene climate pulses in studies using different proxies. The Holocene climate of the Mediterranean has been particularly well investigated, yielding much palynological, speleothem, lake isotope and lake level data (e.g., Allen et al., 2002; Brayshaw et al., 2010; Bar-Matthews and Ayalon, 2011; Magny et al., 2011, 2012; Roberts et al., 2011; Zanchetta et al., 2012; Peyron et al., 2013). These data show a complex pattern of climatic change across the Mediterranean during the Holocene, with strong spatial and temporal variability.

In particular, Magny et al. (2011, 2012) and Peyron et al. (2013) focused on contrasting hydrological patterns for lakes in Italy during the Holocene and suggested dividing these Holocene climatic regimes into northern-central and southern Mediterranean sites. The northern sites show warmer drier conditions during the early to mid-Holocene, but cooler wetter conditions were reconstructed for the sites in southern Italy for the same period. This pattern is reversed in the late Holocene (during the 5000–4000 cal. y BP interval), with warmer drier conditions at the southern sites and cooler wetter conditions at the northern sites.

De Santis and Caldara (2015) proposed a change in the mean pressure configuration in the central Mediterranean during the period between 5500 and 4500 cal y BP.

Roberts et al. (2011) and Brayshaw et al. (2010) suggested an east–west division in Mediterranean climate history. These authors indicate that the eastern Mediterranean experienced an increase in winter precipitation during the early Holocene, followed by an oscillatory decline after c. 6000 cal y BP. In the western parts of the Mediterranean, maximum increases in winter precipitation occurred during the mid-Holocene, approximately 6000–3000 cal y BP, before declining to present-day values.

The records show four main climatic events during the Late Holocene: the Little Ice Age, the Medieval Warm Period, the Dark Age Cold Period, and the Roman Warm Period. These events are believed to be associated with changes in solar activity (Bond et al., 1997, 2001) and in the variability of El Niño events (Moy et al., 2002). However, the influence of climate pulses on the dynamics of the Holocene plains is a challenging topic considering their response to present-day climate change. Holocene coastal plains are among the most populated regions worldwide, so understanding their response and modifications to the most recent climatic pulses can help to understand their future responses to similar events.

In recent times, many work highlighted the importance of the analysis of Holocene coastal plains in the Mediterranean to investigate the complex relationships between tectonics, sea-level changes, sediment supply and anthropic impact on the evolution of this kind of fragile and strategic landscape (Sacchi et al., 2014; Melis

et al., 2018; Cacciari et al., 2020; Lopez-Belzunge et al., 2020; Giaime et al., 2022; Karymbalis et al., 2022).

This work was inspired by the inadvertent exhumation of three ancient tree trunks by local farmers who, while preparing farmland for cultivation, had dug holes about 4 m deep. This study aims to explore possible relations between Holocene climate fluctuations and phases of construction of a deltaic strandplain in a coastal sector of the Tavoliere di Puglia plain in southern Italy.

2 Geomorphological and geological setting of the study area

The Apulian Tavoliere is the second-widest plain in Italy, after the Po Plain. It covers an area of 4,300 km² and is bounded in the north by the Gargano Massif, to the west by the Mountains of Daunia, to the south by the Murge Highlands, and to the east by the Adriatic Sea. It looks like a monotonous flat expanse, tilted on average of a few degrees towards east–northeast, and almost completely lacking in morphological relief, except for very low scarps, bordering terraced marine or alluvial deposits, and erosive furrows of mostly seasonal streams that descend from the Apennine Mountains.

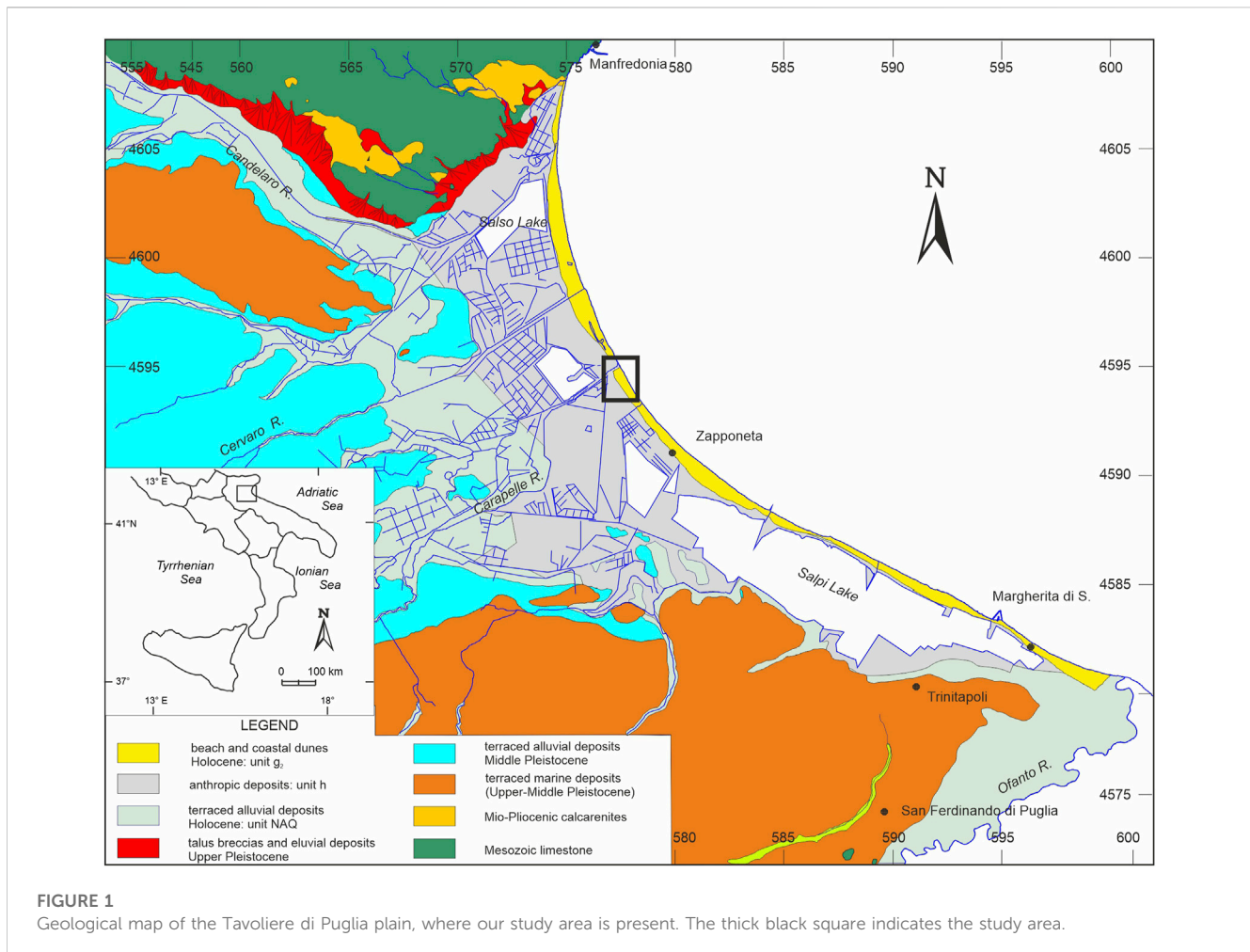
The current morphological structure of the Tavoliere di Puglia began to take shape in the Middle Pleistocene with a generalised uplift, closure of the sedimentary cycle of the Bradano Foredeep and consequent general regression of the sea to its current position (Ricchetti et al., 1992; Doglioni et al., 1994, 1996). Periods of stagnation in uplift and glacial–eustatic oscillations in sea level have created a series of marine and alluvial terraces across the plain (Boenzi et al., 1992; De Santis et al., 2010, 2013). This is characteristic of all Apulian floodplains (De Santis et al., 2020c).

Three terraced surfaces with outcrops of marine or alluvial deposits are recognised above the Holocene and present-day coastal plain in the coastal sector of the Tavoliere di Puglia—the one closest to the Gulf of Manfredonia (Figure 1).

Two main units crop out on the Holocene coastal plain (De Santis et al., 2010, 2013; Caldara et al., 2022). These are the Masseria Inacquata Synthem (NAQ) and beach deposits (g₂), both of which are partially covered by anthropogenic deposits (h).

The Masseria Inacquata Synthem (NAQ) consists of alluvial deposits transitioning towards the coast to submerged beach deposits. The alluvial deposits consist mainly of dark brown to grey or yellowish clays, sands and silts, often with plane-parallel to wavy laminae in the sandy and silty levels. The sedimentation environment is a low-energy alluvial plain with overbank episodes. Towards the east, the unit presents marine-coastal deposits covered by beach deposits (g₂) and/or anthropogenic deposits (h). The marine-coastal deposits of the unit NAQ consist of fine to coarse light grey sands, with interbedded levels of siliceous pebbles of Gargano origin (De Santis and Caldara, 2015). The recognised fossiliferous associations indicate a typical shallow infralittoral environment. The thickness of the unit varies from a few metres along the minor watercourses to a maximum of about 15 m (in drilling) in the sectors closest to the present shoreline. These—particularly the alluvial phase—were dated to the Holocene era due to the post-Würmian sea level rise (De Santis and Caldara, 2016).

The beach deposits (g₂) rest on the Masseria Inacquata Synthem (NAQ) and outcrop roughly along a narrow coastal strip located east of



the coastal road SS n. 159. To the west of this road, the unit tapers inwards and is in turn covered by successive anthropogenic deposits (h). Unit g_2 is composed of an outcrop of greyish marine sands deposited in an emerging beach and coastal dune environment. At depth, the sands alternate with silty-clayey levels, with these becoming thicker and more frequent than the sands with depth. The unit as a whole can be dated to the last millennia of the Holocene, and therefore to the current high sea level phase (De Santis and Caldara, 2015, 2016).

The units NAQ and g_2 were correlated with transgressive (TST) and highstand (HST) deposits, respectively, identifiable on the adjacent continental shelf of the Manfredonia Gulf (De Santis and Caldara, 2015, 2016; De Santis et al., 2020a, 2020b). HST, in the offshore area of the Manfredonia Gulf, rests above a regional downlap surface, or maximum flooding surface (MFS) that marks when the maximum landward shoreline shift occurred. This was approximately 5.5 cal. ka BP during the end of the late Pleistocene-to-Holocene sea-level rise (Correggiari et al., 2001; Cattaneo et al., 2003; Maselli and Trincardi, 2013). Thus, HST and its inland counterpart g_2 are younger than 5.5 cal. ka BP. The maximum thickness of unit g_2 is approximately 25 m (HST in Amorosi et al., 2023).

According to Caldara and Pennetta (1992), Boenzi et al. (2001), and Di Rita et al. (2011), since the sea level stabilised at more or less its current position (i.e., after 5.5 cal. ka BP), the existing and recent coastal plain was affected by the presence of vast lagoonal areas that stretches

between the Gargano Promontory and the Ofanto River. According to Schmiedt (1973), Caldara et al. (2002), and Boenzi et al. (2006), during the Roman period two well defined coastal lakes formed in the coastal area of Tavoliere di Puglia. These were a larger one to the south (Salpi Lake) and a smaller one to the north (Salso Lake). Few studies have assessed the condition of the two lakes during the subsequent Middle Ages. Even after the Middle Ages, these two lakes remained more or less stable, and their shape changed very little until the end of the 18th century and the first two decades of the 19th century (Caldara and Pennetta, 1992; Boenzi et al., 2006).

Later, the area underwent extensive hydraulic drainage and land reclamation (De Santis et al., 2018; 2023a). The history of reclamation in the Tavoliere di Puglia area began with the Regno di Napoli (1806–1815) when the area was ruled by Giuseppe Bonaparte. The territory was dramatically transformed by the law of the 2nd August 1806 that abolished the feudal and ecclesiastical systems. Subsequent division of the demesnes to the settlers paved the way for the reclamation of marshy areas. In 1807, Giuseppe Bonaparte allocated between 17% and 25% of state revenues to carrying out the first land reclamation projects in the Regno di Napoli (Dibenedetto, 1988). The extensive drainage and reclaiming interventions of the Regno delle due Sicilie during the rule of Borbone between 1815 and 1861 continued with the establishment of the Regno d'Italia in 1861, when the responsibility passed to the Genio Civile del Regno d'Italia. Land reclamation became more intense in the



FIGURE 2

Photographs of the exhumed trunks. (A–C) AL1. (D–G) AL2. (H,I,L,M) AL3. For explanations see the text.

20th century when many extensive projects were implemented after the passing of several land management laws. Examples of these include the Serpieri–Iandolo Law of 1933; the Project for Agrarian Transformation Law of 1938; and the Project for Land Transformation Law of 1948.

Since 1934, reclamation work has been overseen by the Capitanata Land Reclamation Consortium. Most of the area under investigation coincides with the area that has been most extensively reclaimed since the 19th century. The extensive reclamation and hydraulic drainage works have

TABLE 1 ¹⁴C datings.

	Sample ID	Laboratory ID	Material	Radiocarbon age	pMC	δ ¹³ C, ‰	Calibrated age
PR12	PR12-3.28	FTMC-HO74-5	Seeds	2988 ± 29	68.94 ± 0.17	-24.19	1301–1119 cal BC
PR11	PR11-2.38/2.40	FTMC-HO74-9	Plants; Seeds	2015 ± 27	77.81 ± 0.22	-26.7	55 cal BC-77 cal AD
	PR11-3.84/3.86	FTMC-HO74-8	Seeds	2123 ± 28	76.78 ± 0.18	-24.75	201–51 cal BC
	PR11-5.41	FTMC-HO74-9	Plants; Seeds	3571 ± 29	64.11 ± 0.12	-23.84	1983–1876 cal BC
PR5	PR5-2.7/2.8	FTMC-HO74-11	Plants; Seeds	116 ± 26	98.57 ± 0.25	-27.14	1802–1937 cal AD
	PR5-14.7/14.8	FTMC-HO74-10	Plants; Seeds	2180 ± 28	76.23 ± 0.21	-24.88	363–152 cal BC
PR4	PR4-3.4/3.5	FTMC-HO74-14	Plants; Seeds	1647 ± 28	81.46 ± 0.16	-14.77	350–480 cal AD
	PR4-20.0/20.1	FTMC-HO74-12	Plants; Seeds	3046 ± 29	68.45 ± 0.16	-21.28	1401–1221 cal BC
AL3	A3S1 EXT	FTMC-HO74-15	Wood	1965 ± 28	78.3 ± 0.16	-25.14	1–125 cal AD
	A3S1 INT	FTMC-HO74-16	Wood	2068 ± 28	77.3 ± 0.25	-23.96	166 cal BC-8 cal AD
AL2	A2S3-2 EXT	D-AMS 045941	Wood	1739 ± 29	80.53 ± 0.20		246–383 cal AD
	A2S3-1 INT	D-AMS 045940	Wood	1975 ± 21	78.2 ± 0.20		3–85 cal AD
AL2	BC	D-AMS 045854	<i>Barnea candida</i>	1816 ± 23	79.77 ± 0.23	0.4	420–610 cal AD

See Figure 5 for the provenance of dated samples.

caused the deposition of the last outcrop in the study area, i.e., the anthropogenic deposits (h).

3 Methods

3.1 Study of tree trunks

3.1.1 Preliminary *in situ* observations: sampling for dating and determination of genus

This work was motivated by the accidental exhumation of three tree trunks during a 4 m-deep excavation in a farmer's field in the coastal area of the Tavoliere di Puglia. Starting from the one closest to the sea and going inland, the three trunks were named AL1, AL2, and AL3 (Figure 2). A qualitative description was made of them, and their diameters and lengths were measured.

They displayed different states of preservation, so AL2 and AL3 were dated because they appeared to be the best preserved and seemed to have the most visible growth rings.

Two samples were dated from each of AL2 and AL3 using the ¹⁴C method. One sample was taken from the innermost zone and one from the outermost zone (Table 1), to reconstruct the maximum chronological range of the trees' ages.

Finally, a gender determination was carried out by Paleoscape Archaeobotanical Services Team (PAST, <http://paleoscapesteam.com>) on four other samples—two for AL1 and one each for AL2 and AL3.

3.2 Definition of the geological–depositional context

3.2.1 Aerial photo analysis and geological setting assessment

First, the extensive existing literature on the geology and geomorphology of the area was consulted (De Santis et al., 2010,

2013, 2014; Caldara et al., 2022; Amorosi et al., 2023; De Santis et al., 2023). Then a study was made of all the aerial photographs covering the study area. The ones that proved particularly useful were:

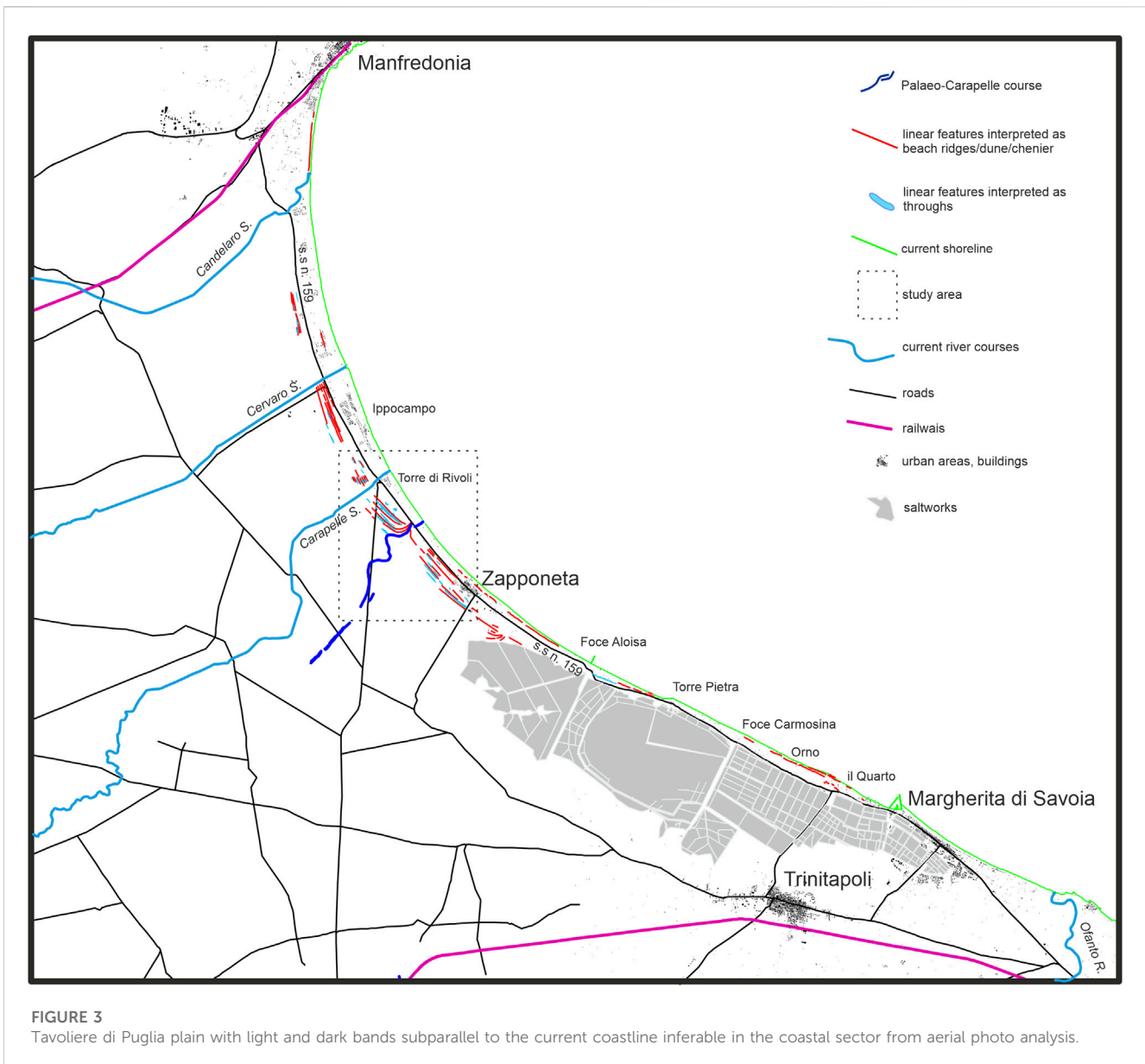
- 1) the 1954 aerial photos provided by the Italian Military Geographic Institute (IGM) in 1954/55 named “G.A.I.—Gruppo Aereo Rilevatore”;
- 2) the 2005 aerial photos provided by Compagnia Generale Ripreseaeree (CGR).

3.2.2 Boreholes

Three continuous boreholes were drilled along an ENE-WSW-oriented section passing through the discovery site of the trunks (Figures 3, 4). The three boreholes were named PR11, PR13, and PR12, from sea to land, and drilled at ca. 1 m of elevation above the present sea level. In addition, cores were recovered *in situ* from two other boreholes drilled as part of works planned for the reconstruction of the bridge over the mouth of the nearby Carapelle Stream. These two boreholes, which were named PR4 and PR5, are located approximately 1.4 km NW of the discovery site of the trunks (Figure 4), and were drilled at ca. 0.3 m of elevation above the present sea level.

3.2.3 Faunal determination and paleoenvironmental reconstruction

Several samples have been collected from the five drill cores and the faunal content has been studied with particular reference to the malacofauna. In the Supplementary Material inherent the five drill cores (PR4, PR5, PR11, PR12, and PR13) all the samples collected are reported; the identificative abbreviation of each sample indicates the borehole from which samples comes and its depth from ground surface. The abundance of mollusc species is qualitatively reported using the abbreviations R, P, C, and F to indicate increasing presence going from R to F. The faunal content has been determined and the sedimentary palaeoenvironments have been defined



according to the manual of Pérès (1967): colours sky blue, yellow and green indicate marine, brackish, and terrestrial species respectively.

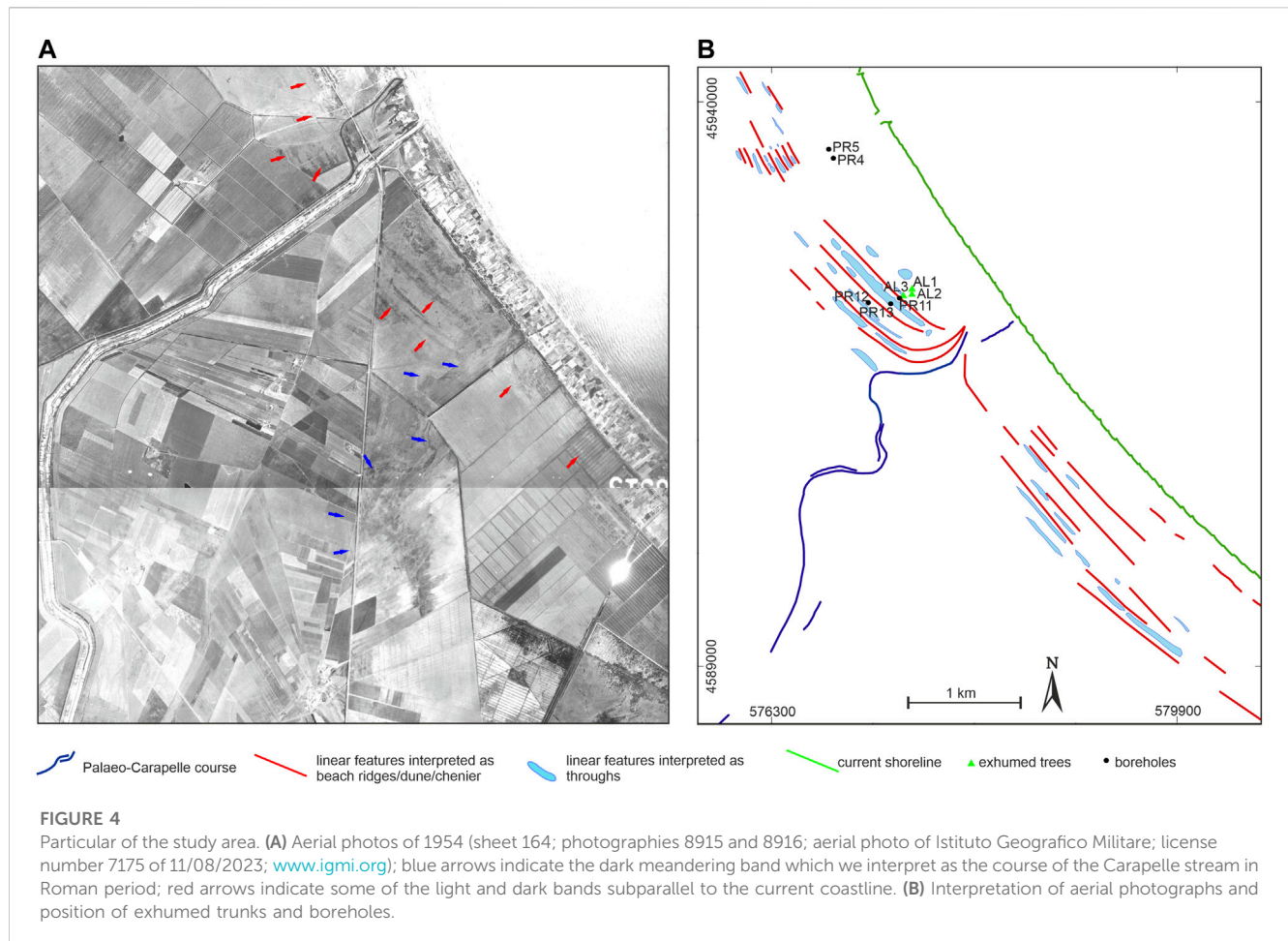
The faunal taxonomy followed is that of the World Register of Marine Species (Worms) (<https://www.marinespecies.org/index.php>).

3.2.4 Dating of samples from boreholes and trunks

Samples of the five drill cores and tree trunks were dated using the ^{14}C method (Table 1) to reconstruct in detail the recent depositional chronology of the area. The samples from cores and AL3 have been analysed by the Vilnius Centre for Physical Sciences and Technology (Vilnius, Lithuania). The equipment used for this analysis was a single-stage accelerator mass spectrometer (SSAMS, NEC, USA), and an Automated Graphitization Equipment AGE-3 (IonPlus AG). The samples were pre-treated with a standard

base–acid–base–acid bleaching protocol. IAEA C3, OXII and IAEA C9 were used as reference materials. The calibration curve and the calibrated probability density function were calculated in OxCal v.4.4.4 (Bronk Ramsey, 2021) using atmospheric data from Reimer et al. (2020).

The samples coming from AL2 and the *Barnea candida* (Linneo) colonising it have been analysed by the DirectAMS radiocarbon dating service in Botell (WA), United States. Here, Accelerator Mass Spectrometers (AMS) NEC Pelletron 500 kV have been used to measure ^{14}C isotopes for radiocarbon dating analysis. Samples were divided into subsamples for chemical pre-treatment, which was achieved using a standard base–acid–base–acid bleaching protocol. Raw measured isotope ratios were transferred to proprietary data analysis software, where final calculations were performed. An aggregate carbon ratio and calculated radiocarbon age were reported after meeting statistical acceptance criteria. The



calibration curve and the calibrated probability density function were calculated in CALIB Radiocarbon Calibration (Stuiver and Reimer, 1993) using atmospheric data from Reimer et al. (2020).

3.2.5 Tephrostratigraphy

Scanning electron microscopy (SEM; LEO EVO-50XVP Zeiss, Cambridge, Cambridgeshire, United Kingdom) coupled with energy dispersive spectrometry (Oxford-Link Ge ISIS energy dispersive spectrometer (EDS) equipped with a super atmosphere thin window) was used at the Dipartimento di Scienze della Terra e Geoambientali (University of Bari, Italy) to investigate the presence of tephra layers (see following Section 4.3.2.1). Samples were wet-sieved, dried, mounted in epoxy resin, polished, carbon-coated and observed with Back Scattered Electrons (BSE) with a 15 kV accelerating potential, and 500 pA probe current. Major elements analyses of tephra fragments were obtained by converting the X-ray intensities of the EDS spectrometer to wt% oxides by the ZAF4/FLS quantitative analysis software of Oxford-Link Analytical (United Kingdom). The accuracy of the analytical data was checked using standard minerals manufactured by Micro-Analysis Consultants Ltd. (United Kingdom). Analytical precision was 0.5% for concentrations N15 wt%, 1% for concentrations of about 5 wt% and 20% for concentrations near the detection limit. The detection limit depends on the considered element, but it is never below 1,000 ppm (Caggiani et al., 2015).

3.2.6 Archaeological studies

The archaeological finds that were analysed came from a depth of between one and 4 m below ground surface. The complete list of the ceramic remains found in Samples A and B is in the Supplementary Material (ARCHEO).

The samples of the ceramic material from the excavation were studied by applying a consolidated approach to ascertain dates and provenance (Sinopoli, 1991; Ceci and Valenzani, 2016). The approach was based on 1) classification and quantification analysis of the finds and 2) comparative assessment with other ceramic samples documented in the regional context.

- (1) The ceramic finds were classified by sorting, pattern detection, and observing characteristics such as paste, decoration and shape, to identify the corresponding industry. The amount and relative weight of the finds for each ceramics type class were then measured, documentation sheets were compiled, and the diagnostic fragments were drawn.
- (2) A literature review was conducted to search for similar samples in the regional context to define places and chronologies of production and diffusion of the identified typologies. In particular, the analysis of the presence and frequency of similar ceramic types and samples allowed for estimating a date for the artefacts.

The archaeological studies supported the interpretation of data and the reconstruction of the paleo-landscape by an integrated methodology that included the historical-topographical analysis of the area (Dall'Aglio, 2000; Renfrew and Bahn, 2016; Ferrari, 2017; Zingaro and Mastronuzzi, 2017; Zingaro et al., 2021).

3.2.7 Palaeobotanical studies

Vegetal remains (mainly seeds) were first extracted by manual cleaning and then observed with a Zeiss Stemi 2000-C stereoscope. We referred to Bojňanský and Fargašová (2007) and the Digital Plant Atlas (<https://www.plantatlas.eu/repository>) for identification.

4 Data and interpretation

4.1 The exhumed trunks

Figures 3, 4 show where the three trunks were found in the context of the study area. The three trunks were named AL1, AL2, and AL3, starting from the one closest to the sea and going inland (Figure 4; Table 1).

AL1 consists of four stem portions ranging from 2 to 2.5 m in length and 30 to 50 cm in diameter (Figure 2A). The state of preservation does not make it possible to define whether the portions are from the same stem. The surface of the samples shows extensive cracking so it is not possible to identify with certainty whether they correspond to the rhytidome or a deteriorated sapwood layer. Woody portions emerge from the stem, referable to remnants of branches or to an outgrowth that is generally associated with a tumour mass or with the area of epicormic branch regrowth along the stem (Figures 2B, C). Wood samples taken for observation purposes show fibre that is flaked, torn and twisted in several places.

AL2 consists of a single sub-cylindrical stem, 5 m long with a diameter of between 64 and 62 cm (Figure 2D). Branching sketches can be identified at one end of the stem. The size, direction and structure of the branching are probably related to the main branches of the crown (Figure 2E). It is unlikely that the branching corresponds to the root system because the transition zones of the woody fibre from the stem to the roots (collar zone) cannot be identified. The surface part of the stem is fissured. The woody fibre of the surface plates does not allow us to define with certainty whether it is part of the rhytidome or the sapwood in a poor state of preservation.

The samples taken for observation show good wood integrity characteristics, with good visibility and serration of the annual rings (Figure 2F) but there is much moist and flaky wood fibre.

AL2 is partially covered by light grey clays containing *Cerastoderma glaucum* (Bruguere), *Abra segmentum* (Recluz); in addition, AL2 is colonised by specimens of *Barnea candida* (Linneo) (Figure 2G) and encrusted by the serpulids *Spirobranchus triqueter* (Linneo), and *S. lamarcki* (Quatrefages), which are, in turn, covered by the bryozoan *Conopeum seurati* (Canu).

AL3 consists of a single sub-cylindrical stem that is more irregular than AL2. It is 5 m long and about 60 cm in diameter (Figure 2H). The samples taken for observation show cracked wood fibre, but exhibit good wood integrity characteristics, with good visibility and serration of the annual rings (Figure 2I). Along the stem there are areas of browning presumably due to combustion

(Figure 2L). In the middle of the stem is a structure that could be referable to a bifurcation of the main stem or a main branch. AL3 is partially encrusted with grey sands containing fragments of marine mollusc shells and encrusted with barnacles (Figure 2M).

From the analysis of genus determination, it was found that "AL1, AL2, and AL3" were identified as probably *Populus* (poplar) based on the presence of a diffuse porous distribution of vessels, alternate intervessel pitting, simple perforation plates, and homocellular (all procumbent) rays with large vessel-ray pits, especially in the marginal rows. The wood also exhibited uniseriate rays but many of the ray cells were somewhat deteriorated, and it could not be determined with certainty that all of the rays were uniseriate.

4.2 Evidence from aerial photographs

Aerial photographs, particularly those of 1954 and 2005, indicated the existence of numerous buried features attributable to the upper part of unit g₂ (De Santis et al., 2010, 2013; Caldara et al., 2022) immediately underneath the thin cover of the Anthropogenic Deposits (h). These features are represented by alternating light and dark bands subparallel to the current coastline. They are present along the entire coastal strip of the Tavoliere di Puglia (Figure 3) but, in the central area, they increase in number and are arranged to the right and left of a dark meandering band that stretches from the hinterland almost to the coast (Figure 4).

From an analysis of the data in the literature, we can exclude with certainty that the dark meandering band is attributable to the course that the Carapelle stream has taken in recent historical times (De Santis et al., 2023).

4.3 Geological units and reconstruction of depositional environments

The stratigraphy, depositional environments, and chronology of the study area were interpreted by: 1) studying boreholes PR4, PR5, PR11, PR12, and PR13 (Figures 4, 5); 2) results from the carbon dating (Table 1); 3) analysis on the two levels of tephra present in PR12 and PR11 (Figures 5–7; Table 2); 4) archaeological and palaeobotanical analyses (Figures 8, 9); and 5) analysis of data in the literature. The main units recognised are the same as those already recognised, in their general lines, in the study area (Caldara et al., 2022). However, thanks to the new data, they are described in more detail in this study, as they occur in the study area, from bottom to top.

4.3.1 Unit NAQ

Deposits of the unit NAQ have been found at depths between about 25 and 30 m below ground surface, which were reached only by drilling PR4 and PR5. These can be correlated with the TST present in the southern Adriatic and the Manfredonia Gulf (De Santis and Caldara, 2016; De Santis et al., 2020a, b). They consist mainly of clay and silty clay and contain a rich marine fauna consisting of *Turritellinella tricarinata* (Brocchi), *Kurtiella bidentata* (Montagu), *Nucula nitidosa* (Winckworth), *Abra nitida* (Müller), *Antalis inaequicostata* (Dautz) and *Corbula gibba* (Olivieri). Many ossicles of Asteroidea and vertebrae of Ophiuroidea were found.

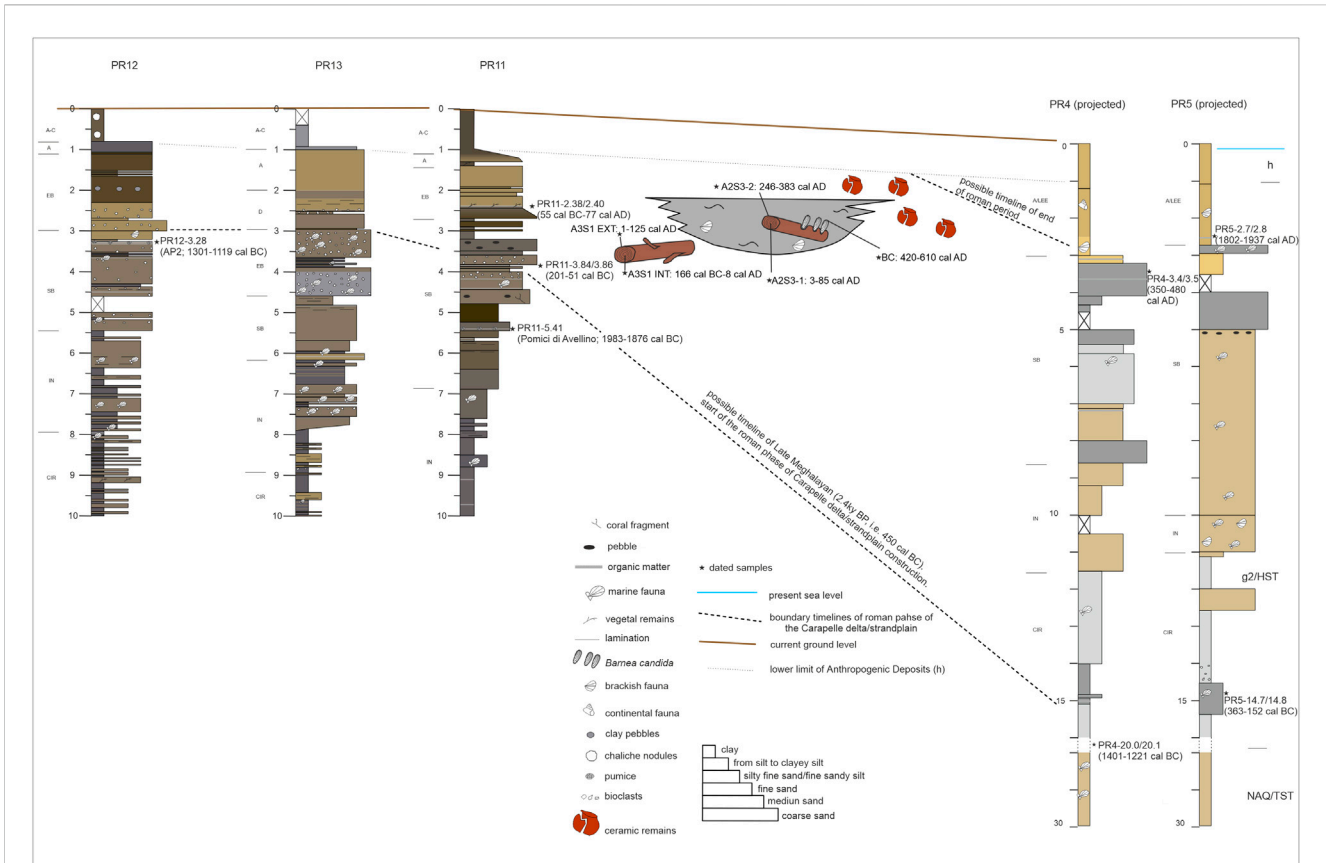


FIGURE 5

Geological section across the study area. CIR, circalittoral; IN, infralittoral; SB, submerged beach; EB, emerged beach; D, dune; A, alluvial; A–C, alluvial, anthropic filling; LEE, euryaline and eurythermal lagoon. Only dated samples have been reported. All samples for each borehole are reported in the [Supplementary Material](#).

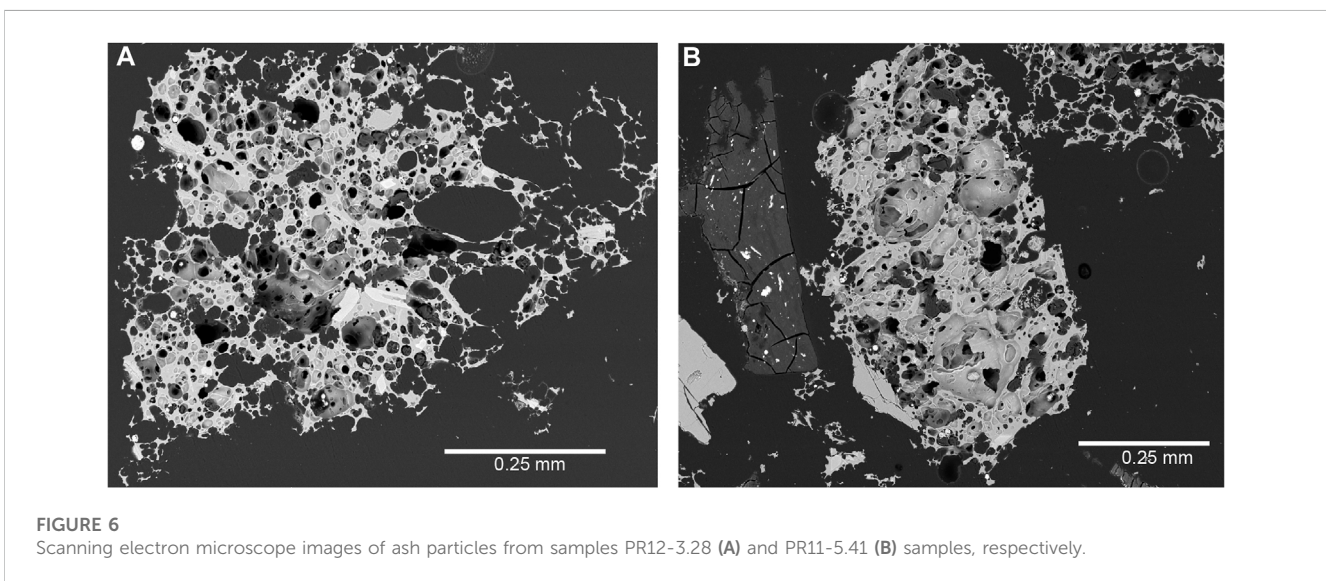


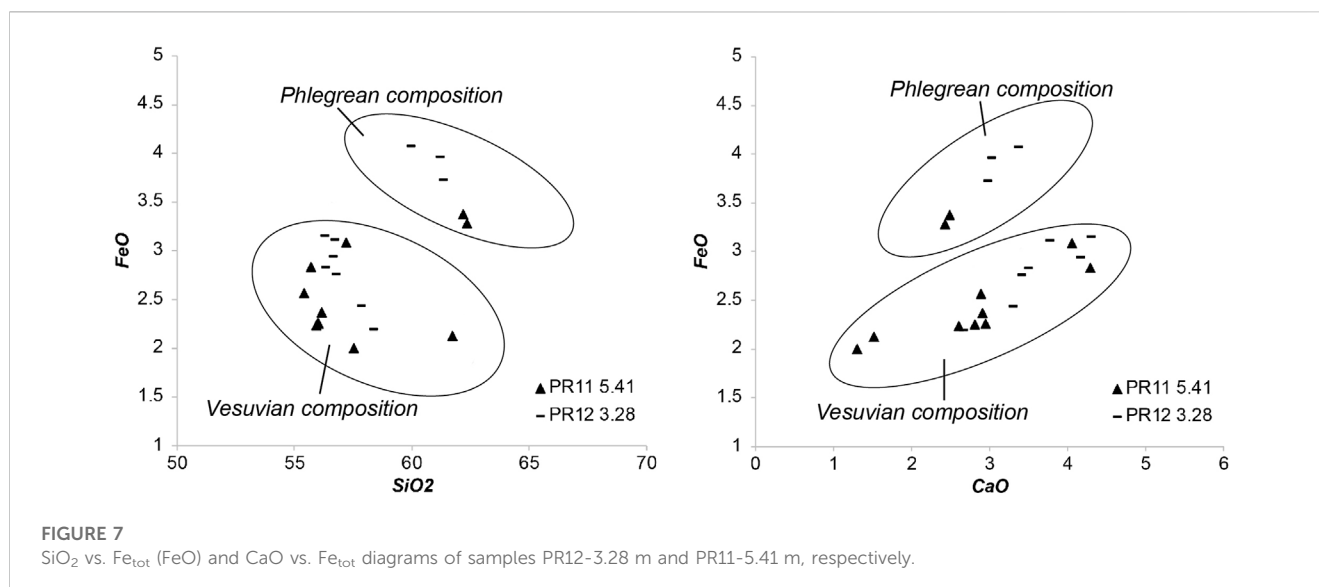
FIGURE 6

Scanning electron microscope images of ash particles from samples PR12-3.28 (A) and PR11-5.41 (B) samples, respectively.

4.3.1.1 Interpretation of unit NAQ

The fauna of the NAQ unit in the study area indicates a circalittoral environment with a biocoenosis comparable to that of the terrigenous mud (VTC) (*sensu* Pérès, 1967), which had

already been well documented in the Adriatic Sea (Vatova, 1949; Pérès et al., 1964). The unit NAQ in the study area has been interpreted as a set of deposits referable to bay or estuarine environments, deposited during the last Holocene transgression



within incised valleys whose formation dates back to the previous lowstand of MIS 2 (De Santis and Caldara, 2016; Amorosi et al., 2023). The age is thus part of the Holocene before 5.5 cal. ky BP (Trincardi et al., 1996; Cattaneo et al., 2003; Maselli and Trincardi, 2013; De Santis et al., 2020a, b).

4.3.2 Unit g₂

Deposits of unit g₂ are found from the base of h down to about 20–25 m below ground surface. These can be correlated, offshore, with the HST found in the southern Adriatic and the Manfredonia Gulf (Trincardi et al., 1996; Cattaneo et al., 2003; Maselli and Trincardi, 2013; De Santis and Caldara, 2016; De Santis et al., 2020a, b). From a lithological point of view, these deposits consist of a dense alternation of clayey and silty layers in the lower levels. Towards the top, a sandy component begins to appear, at first fine and then medium-coarse. This initially alternates with the clayey-silty levels, and then becomes preponderant or exclusive. Laterally, sands can transition to grey clayey-silty deposits rich in *Cerastoderma glaucum* (Bruguiere) and *Abra segmentum* (Recluz); AL2 was found in these deposits (Figure 5).

The deeper clayey part, from bottom core to ca. 20 m in depth in PR4 and PR5, is rich in marine fauna consisting of *Kurtiella bidentata* (Montagu), *Corbula gibba* (Olivi), *Nucula nitidosa* (Winckworth), *Turritellinella tricarinata* (Brocchi), *Lembulus pella* (Linneo), *Abra nitida* (Müller), *Pitar rudis* (Poli), and *Antalis inaequicostata* (Dautz). Many ossicles of Asteroidea and vertebrae of Ophiuroidea were present.

The faunal content is scarce in PR4 and PR5 from bottom core to ca. 11.5 m, in sediments of mainly clay to silty clay or from silt to clayey silt rich in vegetal remains. *Corbula gibba* (Olivi), *Nucula nitidosa* (Winckworth), *Abra alba* (Wood), and *Abra nitida* (Müller), and also vertebrae of Ophiuroidea were found. A similar faunal association was found in PR12, PR13 and PR11, from bottom core to ca. about eight, nine and 10 m, respectively.

Upwards in all boreholes, with the increase of the sandy component, the palaeocommunities are characterised by stocks of

Psammophilous species, mostly *Chamelea gallina* (Linneo), *Spisula subtruncata* (Da Costa), and *Peronidia albicans* (Gmelin), and subordinately *Lentidium mediterraneum* (Costa), *Abra tenuis* (Montagu), *Donax semistriatus* (Poli), *Donax trunculus* (Linneo), and pelophilous species such as *Loripes orbiculatus* (Poli), *Hydrobiidae* spp., *Pirenella conica* (Blainville), and *Pusillina lineolata* (Michaud). There is also a stock of species typical of unstable sedimentary conditions such as *Corbula gibba* (Olivi), *Fustiaria rubescens* (Deshayes), and *Moerella distorta* (Poli) or herbivorous algal detritus-feeders such as *Tricolia pullus* (Linneo), *Rissoidea* spp., and *Trochidae* spp.

Starting from 3.28, 4.40, and 2.60 m respectively in PR12, PR13 and PR11, medium and coarse bioclastic sand prevails, characterised by heavily worn and fragmented mollusc remains with rare benthic foraminifera. In PR4 and PR5, at depths of about 2.70 and 1.90 m respectively, sedimentary levels are characterised by *Cerastoderma glaucum* (Bruguiere), *Hydrobiidae* spp., and *Characeae oogons* or by *Ovatella myosotis* (Draparnaud) and Pulmonata.

Exclusively continental faunas, such as *Trochoidea trochoides* (Poiret), *Pomatias elegans* (Müller), and *Hohenwartiana hohenwarti* (Rossmässler) are found from depths of 1.05, 2.0, and 1.35 m, respectively in PR12, PR13 and PR11.

Radiocarbon dating shows that the age of the part of g₂ intercepted by the boreholes ranges from a maximum of 1983–1876 cal BC to a minimum of 1802–1937 cal AD (Figure 5), thus to the Holocene.

4.3.2.1 Tephrostratigraphy of unit g₂

The tephrostratigraphical study was carried out only within unit g₂ because it is connected with the surface linear features detected by the aerial photo analysis, and it was the unit hosting the three exhumed trunks. Two tephra layers were recognised at 3.28 and 5.41 m in the PR12 and PR11 cores, respectively (Figures 5, 6). These are inside the g₂ unit.

The chemical composition (Figure 7; Tab. 2) of ash particles in both samples, coupled with the reconstructed spatial dispersion of

TABLE 2 EDS analyses of glasses from samples PR12-3.28 m (a) and PR11-5.41 m (b).

PR12_3.28m	1	2	3	4	5	6	7	8	9	10	
SiO ₂	61.22	56.78	56.66	56.32	59.99	56.30	57.87	61.36	56.71	58.38	
TiO ₂	0.52	0.26	0.38	0.30	0.53	0.40	0.26	0.52	0.35	0.00	
Al ₂ O ₃	18.32	21.62	21.29	21.59	18.42	21.24	21.83	18.59	21.50	22.43	
FeO	3.96	2.76	2.94	2.83	4.07	3.15	2.44	3.73	3.11	2.19	
MnO	0.00	0.00	0.00	0.19	0.19	0.21	0.00	0.00	0.00	0.18	
MgO	0.81	0.26	0.44	0.29	0.88	0.36	0.20	0.80	0.40	0.24	
CaO	3.03	3.41	4.17	3.50	3.37	4.30	3.30	2.98	3.77	2.67	
Na ₂ O	3.08	5.67	4.84	5.63	3.10	5.02	5.32	2.89	5.34	5.92	
K ₂ O	8.40	8.27	8.21	8.40	8.83	7.97	7.70	8.34	7.92	6.63	
P ₂ O ₅	0.00	0.00	0.15	0.00	0.00	0.22	0.00	0.14	0.00	0.00	
F	0.00	0.36	0.30	0.32	0.00	0.20	0.29	0.00	0.31	0.72	
Cl	0.65	0.60	0.62	0.63	0.62	0.62	0.61	0.64	0.58	0.64	
SO ₃	0.00	0.00	0.00	0.00	0.00	0.00	0.18	0.00	0.00	0.00	
Total	99.99	99.99	100.00	100.00	100.00	99.99	100.00	99.99	99.99	100.00	
K ₂ O/Na ₂ O	2.73	1.46	1.70	1.49	2.85	1.59	1.45	2.89	1.48	1.12	
PR11_5.40m	1	2	3	4	5	6	7	8	9	10	11
SiO ₂	56.17	56.01	55.42	55.95	56.04	55.72	57.21	62.37	57.53	61.75	62.20
TiO ₂	0.23	0.18	0.23	0.23	0.19	0.27	0.35	0.49	0.00	0.17	0.54
Al ₂ O ₃	21.95	21.97	21.68	22.05	22.08	21.27	21.48	18.38	23.92	21.42	18.51
FeO	2.37	2.26	2.56	2.23	2.25	2.83	3.08	3.28	2.00	2.12	3.37
MnO	0.00	0.00	0.00	0.20	0.00	0.00	0.23	0.00	0.20	0.27	0.00
MgO	0.29	0.20	0.15	0.19	0.22	0.36	0.45	0.51	0.47	0.13	0.59
CaO	2.91	2.95	2.89	2.61	2.81	4.29	4.06	2.43	1.30	1.52	2.49
Na ₂ O	7.47	7.66	7.18	7.80	7.74	6.08	4.79	3.56	6.85	5.18	3.15
K ₂ O	7.38	7.46	8.49	7.51	7.53	8.06	7.41	8.22	6.20	6.47	8.45
P ₂ O ₅	0.00	0.00	0.00	0.00	0.00	0.15	0.00	0.00	0.00	0.00	0.00
F	0.65	0.66	0.76	0.59	0.54	0.33	0.30	0.00	0.89	0.28	0.00
Cl	0.59	0.66	0.64	0.64	0.59	0.63	0.64	0.75	0.64	0.68	0.72
SO ₃	0.00	0.00	0.00	0.00	0.00	0.00	0.00	0.00	0.00	0.00	0.00
Total	100.01	100.01	100.00	100.00	99.99	99.99	100.00	99.99	100.00	99.99	100.02
K ₂ O/Na ₂ O	0.99	0.97	1.18	0.96	0.97	1.33	1.55	2.31	0.91	1.25	2.68

eruptive ash, is compatible with two explosive events of Somma–Vesuvius (Italy). These are the Avellino pumice of 3900 cal y BP (Sulpizio et al., 2010; Sevink et al., 2011) and/or the AP2 eruption of between 3680 ± 190 and 3170 ± 240 cal yr BP (Arnò et al., 1987; Rolandi et al., 1998; Andronico and Cioni, 2002; Santacroce et al., 2008). In particular, the component referable to the Avellino pumice eruption can be identified in white pumices and in the abundance of coarse particles, from coarse ash

(0.5–2.00 mm) to fine lapilli (2.00–4.00 mm) (Sulpizio et al., 2010). Both samples also show little contamination of the Phlegraean volcanic area (Figure 7). The attribution to the Avellino pumice and/or AP2 eruption of two of the studied samples suggests that contamination came from volcanic activity between 4400 and 3500 cal y BP (Smith et al., 2011), probably the Astroni 6 eruption (Isaia et al., 2004; Mele et al., 2020).

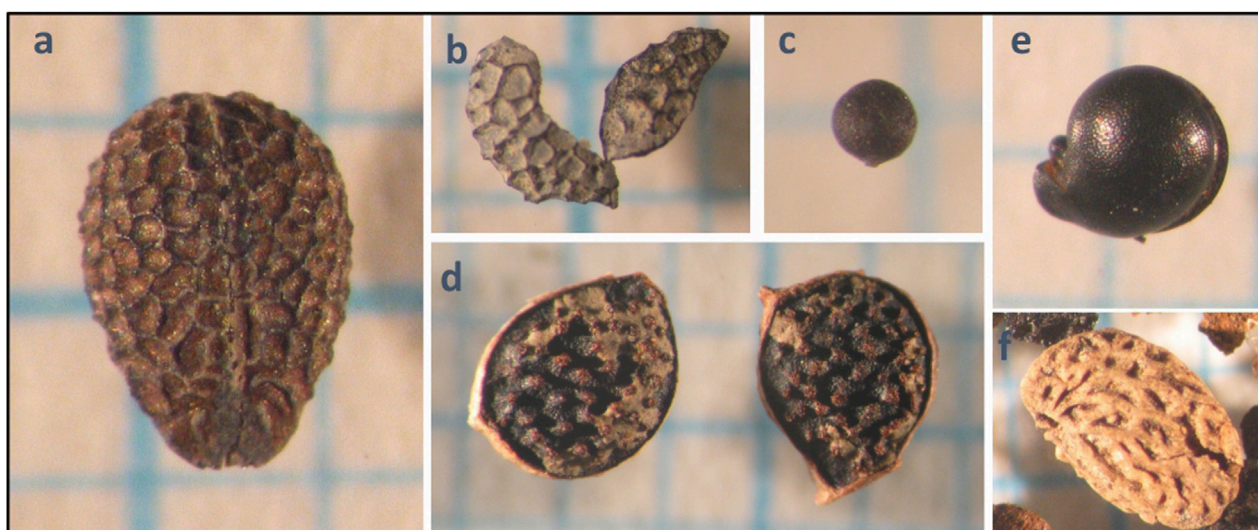


FIGURE 8

Seeds of taxa referable to sinanthropic environments: (A) *Euphorbia* cf. *helioscopia*; (B) *Papaver* sp.; (C) *Sinapis* sp. *Trifolium* cf. *trilobus* (D) indicates humid environments with freshwater; *Suaeda* cf. *maritima* (E) indicates saltmarsh vegetation. (F) *Rubus* sp.

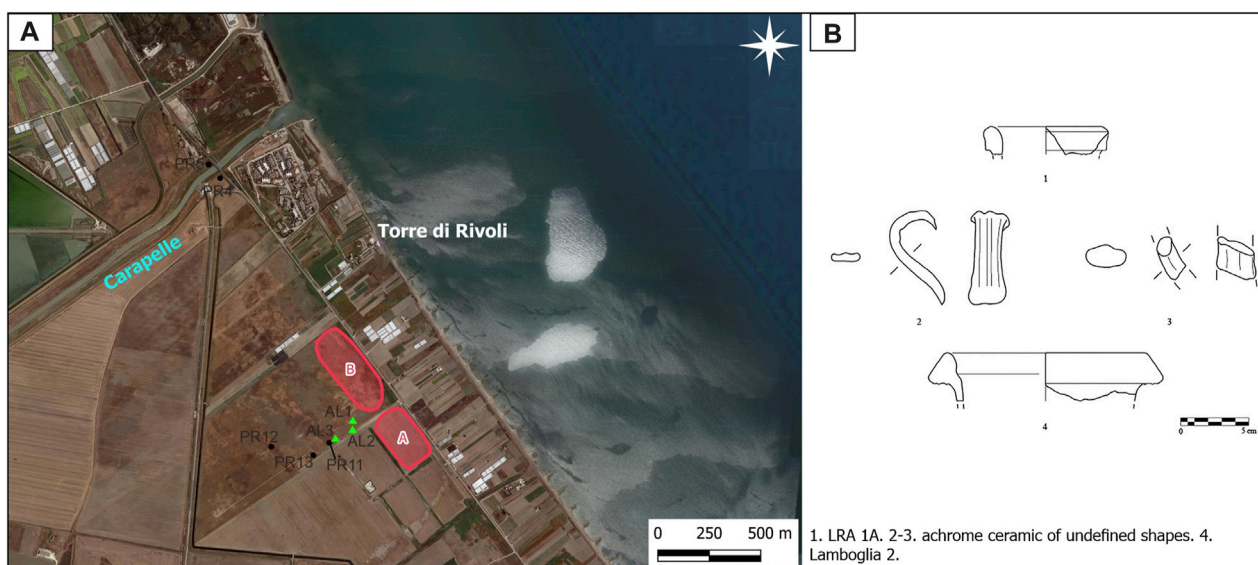


FIGURE 9

(A) Localization of the areas where the archaeological material of Sample A and B was found, along with the position of boreholes studied and sites of trunk exhumation. (B) Graphic documentation of the diagnostic fragments (see the text for abbreviations).

4.3.2.2 Results of palaeobotanical study on samples of unit g₂

The palaeobotanical study has been carried out only within unit g₂ because it is connected with the surface linear features detected by the aerial photo analysis and it was the unit hosting the three exhumed trunks.

The most frequent botanical remains observed (Figure 8) are referred to as *Rubus* sp. Other frequent taxa are *Sinapis* spp., *Brassica* spp., *Chenopodium* spp., *Melilotus* spp., *Medicago* spp., *Trifolium* spp., *Euphorbia* cf. *helioscopia*, *Papaver* cf. *rhoeas*, and *Suaeda* cf. *maritima*.

In addition, *Papaver* cf. *rhoeas*, *Vitis vinifera*, *Cirsium* sp., *Silene* sp. (cf. *vulgaris*), *Beta* sp. and *Polygonum* sp. were also present. Seeds and leaves of *Populus* sp. were found in borehole PR13. In borehole PR4 at 20 m depth, remains of *Posidonia oceanica* (L.) Delile (1813) have been found.

4.3.2.3 Archaeological finds within unit g₂

The archaeological finds analysed come from depths of between one and 4 m. Thus, they can be allocated in the upper part of unit g₂.

In particular, the ceramic material was found in two distinct areas defined as A and B (Figures 5, 9A, B) and the corresponding finds are referred to as Sample A and Sample B respectively. The complete list of the ceramic remains found in Samples A and B is in the [Supplementary Material](#) ARCHEO.

The archaeological analysis of Sample A revealed the presence of 43 well-preserved sherds corresponding to a total weight of 1,259 g. These were from amphorae of Oriental (28 fragments, 905 g) and African (3 fragments, 165 g) production and to vessels used for canteen and pantry (5 fragments, 124 g) and firing (7 fragments, 33 g) of local/regional and Aegean-Eastern production.

The sherds are fragments of wall, handles or rims. In particular, we report:

- 1) sherds of Late Roman Amphora (LRA) 1 produced in the Roman provinces of Cilicia, Cyprus and Rhodes dating from 390 to 700 cal AD (Pieri, 2005). These sherds are well preserved and similar to those documented in other sites of the Puglia region (De Mitri, 1993; Disantarosa, 2007; Disantarosa, 2010; Disantarosa et al., 2015);
- 2) sherds of LRA 3, produced along the west coast of Cilicia and widespread in the western Mediterranean region between 401 and 600 cal AD (Pieri, 2005), and LRA 4, produced along the southern coast of Palestine between 301 and 700 cal AD (Pieri, 2005);
- 3) sherds presumably corresponding to medium-sized cylindrical vessels (Panella, 2001) produced between 301 and 450 cal AD (Bonifay, 2007);
- 4) a sherd of painted ceramic documented in the region and all of southern Italy dating from 351 to 800 cal AD (Totten, 2022);
- 5) sherds of Aegean-Eastern production presumably belonging to the Late Roman micaceous Aegean Cooking Ware class, which was widespread in the Mediterranean area between 401 and 510 cal AD (Riccatò, 2020).

The archaeological analysis of Sample B yielded 13 well-preserved sherds corresponding to a total weight of 741 g and belonging to amphorae of Italic (2 fragments), Oriental (3 fragments) and African (4 fragments) production, and vessels used for canteen and pantry (3 fragments) and 1 fragment of dolium.

The sherds are fragments of wall, handle or rims. In particular, we report:

- 1) a sherd of Lamboglia 2 produced along the western coast of the Adriatic Sea (Panella, 1998; Bruno and Bocchio, 2005) and widely present in Apulia (Disantarosa et al., 2015) between 150 and 1 cal BC.
- 2) sherds of LRA 1 from between 390 and 700 cal AD (Pieri, 2005);
- 3) sherds presumably corresponding to medium-sized cylindrical vessels from between 301 and 450 cal AD (Bonifay, 2007) and large cylindrical vessels presumably produced between 451 and 700 cal AD (Bonifay, 2004).

The archaeological remains provide an overall chronological indication of the ceramic material being dated between 150 cal BC and 800 cal AD, with greater attested evidence of the historic period of 390–700 cal AD.

4.3.2.4 Overall interpretation of unit g_2 in the context of the Holocene and focus on its upper part

The fauna of the unit g_2 shows, from bottom to top, a transition from circalittoral to infralittoral environments, and then closes the succession with emerged beach and dune environments (Figure 5). The circalittoral environment is represented by biocoenosis of the terrigenous mud (VTC) (*sensu* Pérès, 1967), under unstable sedimentary conditions, typical of the heterogenous association (PE) (*sensu* Di Geronimo, 1984). The infralittoral environments are represented by biocoenosis of fine well-sorted sand (SFBC) (*sensu* Pérès, 1967), and superficial muddy sands in sheltered areas (SVMC) (*sensu* Pérès, 1967), both of which are characterised by taxa indicative of sedimentary instability and, above, by populations of herbivorous, algal detritus-feeders. Locally, a biocoenosis indicative of euryhaline and eurythermal lagoons (LEE) (*sensu* Pérès, 1967) is present.

Finally, the marine environments with biocoenosis of the fine sands in very shallow water (SFHN) (*sensu* Pérès, 1967) are marked by *Lentidium mediterraneum* (Costa). Above this, deposits of emerged beach and aeolian dunes are found in the inner boreholes (PR11, PR13 and PR12), and salt marsh environments with *Ovatella myosotis* (Draparnaud) and LEE with *Cerastoderma glaucum* (Bruguere) are associated with the outer boreholes (PR4 and PR5).

The above-mentioned data are consistent with the sedimentary succession within unit g_2 , showing, on the whole, an upward coarsening trend, which can be interpreted with a coastal delta progradation model (Shepard et al., 1960), and a transition from a pro-delta marine environment to a delta front and delta plain environment. This is analogous to the already-established Holocene evolution of the coastal area of the Tavoliere di Puglia, particularly the coastal region where our study area is located (Amorosi et al., 2023).

The analysis of the stratigraphies of the boreholes shows alternating sub-environments of emerged or submerged beaches in the delta front, while the sub-environments in the delta plain are aeolian dunes, ponds and lagoons.

The attribution, in our study area, of g_2 to a deltaic environment is reinforced and better defined by the linear features inferable from the interpretation of the aerial photographs of the area. Thus, we can better define the palaeoenvironment by interpreting the set of these features as traces of an ancient deltaic strandplain (Otvos, 2000; Fitzgerald et al., 2007; Isla et al., 2023) created at the mouth of the Carapelle Stream, on the surface of which there were sandy ridges (beach ridges and/or aeolian dunes and/or cheniers) alternating with interdune depressions.

The fact that AL2 had been colonised by *Barnea candida* (Linneo), encrusted by *Spirobranchus lamarcki* (Quatrefages), and covered by the bryozoan *Conopeum seurati* (Canu), suggests the existence of brackish ponds or lagoons, characterised by variable and/or reduced salinity (Bianchi, 1981; Occhipinti Ambrogi, 1981). These could have been established within depressions or may have occupied more or less extensive areas of the deltaic strandplain. This conclusion is consistent with the finding of *Cerastoderma glaucum* (Bruguere) and *Abra segmentum* (Recluz) within the clays partially covering AL2. As already mentioned, g_2 can be attributed to the Holocene. However, the uppermost part of g_2 can be chronologically constrained within a narrower period of the upper Holocene. The

lower chronological constraint is provided by the two tephra levels intercepted at 3.28 and 5.20 m below ground surface in boreholes PR12 (the innermost) and PR11 (the outermost and closest to the sea) respectively (Figures 4, 5). Radiocarbon dating on plant remains (samples PR12-3.28 and PR11-5.41; Figure 5; Table 1) in these two sedimentary levels yielded ages of 1301 to 1119 cal BC for sample PR12-3.28 and 1983 to 1876 cal BC for sample PR11-5.41.

The date of sample PR12-3.28 is consistent with the AP2 eruption of Vesuvius, dating back to between 3680 ± 190 and 3170 ± 240 cal yr BP, i.e., 1730 ± 190 and 1220 ± 240 cal BC (Arnò et al., 1987; Rolandi et al., 1998; Andronico and Cioni, 2002; Santacroce et al., 2008). The date of sample PR11-5.41 is consistent with the Pomici di Avellino event of Vesuvius, dating back to 3.9 cal. ky BP, i.e., 1950 cal BC (Sulpizio et al., 2010; Sevink et al., 2011).

The above suggests that the level intercepted at 5.41 m in borehole PR11 is a sedimentary event almost contemporaneous with the Vesuvian Pomici di Avellino eruption; while the level intercepted at 3.28 m in borehole PR12 is a sedimentary event almost contemporaneous with the Vesuvian AP2 eruption (Figure 5). Both events reworked older deposits: Pomici di Avellino and Phlegraean eruptions in the case of the level intercepted at 3.28 m in borehole PR12, and only Phlegraean eruptions in the case of the level intercepted at 5.41 m in borehole PR11.

The second chronological constraint is the fact that the part of the succession stratigraphically above the two layers with Pomici di Avellino and AP2 tephra contains eight dates (samples PR11-3.84/3.86, A3S1 INT, A3S1 EXT, A2S3-1, A2S3-2, BC, and PR4-3.4/3.5) (Figure 5; Table 2) indicating an interval between a maximum of 201 cal BC and a minimum of 480 cal AD, thus allowing this upper part to be attributed to the Roman period. The three exhumed tree trunks are attributable to this time interval (more specifically to the period straddling the birth of Christ) and come from the basal part of the delta plain facies, which is in contact with the underlying delta front facies.

Palaeobotanical analysis, with the abundance of *Rubus* sp., indicates the presence of the alliance of Pruno-Rubion ulmifolii with O. de Bolòs 1954 (Crataego-Prunetea Tx. 1962), i.e., deciduous shrubby mesophytic mantle and seral communities of deciduous forests, mostly of Carpino-Fagetea and Alno glutinosae-Populetea albae forest vegetation, dominated by phanerophytes and nanophanerophytes, which are mainly thorny and prickly shrubs that grow on rich nutrient soils at forest edges, fields, grasslands or river-banks, with Mediterranean to Atlantic distribution (Rivas-Martinez et al., 2002; Mucina et al., 2016). It is worth noting that Alno glutinosae-Populetea albae includes azonal alluvial forests, i.e., riparian wet deciduous woodland and willow communities of the Eurosiberian and Mediterranean regions. Typically, Pruno-Rubion ulmifolii vegetation and, in particular, *Rubus* spp. communities, form the shrubby mantle of riparian forests, e.g., poplar groves and willows. When forest vegetation is removed or severely altered, *Rubus* spp. form secondary vegetation stages (regressive dynamic process) and so tend to expand, often forming extensive mats on the river bed. Moreover, an increase in the abundance of *Rubus* (and other synanthropic and generalist species) is quite common in disturbed riparian forests (Gafta, 1993; Angiolini et al., 2023).

Other abundant taxa, i.e., *Sinapis* spp., *Brassica* spp., *Chenopodium* spp., *Melilotus* spp., *Medicago* spp., *Trifolium* spp., *Euphorbia* cf. *helioscopia*, and *Papaver* cf. *rhoea* indicate some level of anthropisation because most of them are diagnostic species of segetal weeds and ruderal vegetation of human-modified habitats of the Mediterranean (Chenopodieta Br.-Bl. in Br.-Bl. et al., 1952; Fanelli and Lucchese, 1998; Brullo et al., 2007; Brullo and Guarino, 2007; Silc, 2010). The presence of more or less intense human activity is confirmed also by *Cirsium* sp., *Silene* sp. (cf. *vulgaris*), *Beta* sp., and *Polygonum* sp. (Rivas-Martinez et al., 2002; Mucina et al., 2016). Finally, the presence of *Vitis vinifera* in PR 13 is a clear indication of cultivated areas.

It is worth noting that *Ranunculus trilobus* (present only in PR11, where it is abundant) indicates wet areas that may even be periodically submerged by freshwater. It is diagnostic of Mediterranean temporary pond vegetation (Isoetion Br.-Bl. 1936; Tomaselli et al., 2022).

Suaeda cf. *maritima*, which is present in PR11 and PR13, is a diagnostic species of *Thero-Suaedetalia splendentis* Br.-Bl. & O. de Bolòs 1958, i.e., halo-nitrophilous annual pioneer coastal plant communities (Rivas-Martinez et al., 2002; Tomaselli et al., 2020).

4.3.3 Unit h

From the topographical surface up to a maximum of ca. 1 m below the current ground surface, we find Anthropogenic Deposits (h), generally consisting of light grey to dark grey clays, deposited as a result of the anthropogenic action of reclaiming the coastal plain of the Tavoliere di Puglia by landfilling, by controlled flooding, or by drainage through the construction of drainage channels (De Santis et al., 2023).

5 Discussions

The combination of the stratigraphic analysis of the boreholes in the study area, the dating of the upper part of g₂, the interpretation of the aerial photographs, and the palaeobotanical and archaeological evidences lead us to the conclusion that there was a phase of construction of the Carapelle deltaic strandplain referable to the Roman period, after a sedimentary event datable to between 1301 and 1119 cal BC, which was almost contemporaneous with the AP2 eruption of Vesuvius (see borehole PR12 in Figure 5).

On the other hand, ¹⁴C dates after that sedimentary event indicate a maximum possible time range between 201 cal BC and 480 cal AD, if we exclude only the very recent date of 1802–1937 cal AD in the borehole PR5.

Between the age of the sedimentary event dated at 1301–1119 cal BC (see borehole PR12 in Figure 5) and the subsequent available ¹⁴C date of 201–51 cal BC (see borehole PR11 in Figure 5), we can consider the chronology proposed by Susini et al. (2023). These authors report that, starting from 2.4 cal ky BP (ca. 450 cal BC, that is, Late Meghalayan), a strong freshwater influx from the Carapelle River caused the rapid progradation of the floodplain. We interpret this event as the beginning of the Roman-era phase of the Carapelle deltaic strandplain. Therefore, the overall time encompassed by its construction can be reconstructed as 450 cal BC to 480 cal AD (Figure 5).

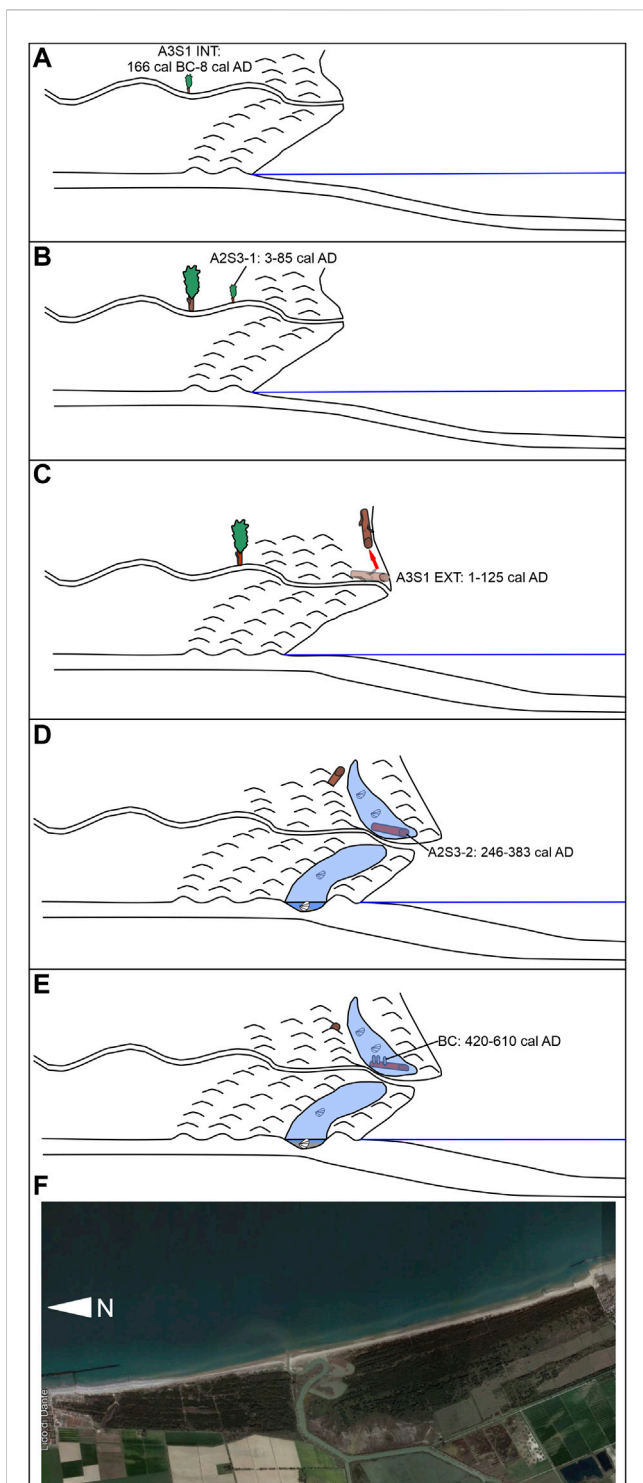


FIGURE 10

Reconstruction of the parallel evolution of the deltaic strandplain and *Populus* trees whose trunks have been exhumed, with dated samples obtained from AL2 and AL3. In this reconstruction the hypothesis that AL2 and AL3 grew in the delta plain is showed. The horizontal blue line represents the sea level. See the text at [Section 5.1](#) for the explanation of the evolutive phases (A-F). Image of (F) by GoogleEarth.

5.1 Reconstruction of the evolution of the Carapelle deltaic strandplain in Roman times

In our reconstructed scenario, the Roman phase of the mouth of the Carapelle stream was accompanied by the formation of a deltaic strandplain (Otvos, 2000) in the area surrounding the mouth. A strandplain, in general, is a belt of sand along a shoreline exhibiting parallel or semi-parallel sand ridges separated by troughs, typical of prograding beaches. Strandplains are typically created by the redistribution of coarse sediment by waves and longshore currents on either side of a river mouth. Thus, they are part of a wave-dominated delta (McCubbin, 1982; Fitzgerald et al., 2007). According to Isla et al. (2023), a deltaic strandplain in particular is controlled by episodic river input of sediment, but other processes such as longshore transport may be equally important in developing progradation of the shoreline. Deltaic strandplains are common along microtidal and mesotidal coasts, having low to moderate wave energy and sand-dominated regimes (Isla et al., 2023). Sand ridges in a strandplain prograde predominantly parallel with or perpendicular to the shoreline, and are formed by longshore drift and current transport, aeolian sand accumulation, or both from littoral and fluvial sources (Otvos, 2022). The strandplain progradation is either continuous or discontinuous. In the latter case, the inclusion of subtidal “cat’s eye” ponds can occur (Otvos, 2000). We identified a “pond” in seaward sector of the Carapelle strandplain (Figure 5) where AL2 was deposited after its death and then colonised by taxa indicative of variable and/or reduced salinity. Because of this we can conclude that a first continuous and then discontinuous deltaic strandplain was built around the Carapelle mouth in Roman times.

The Carapelle deltaic strandplain formed along the coast of the Manfredonia Gulf, a wave-dominated coast fronted by a relatively wide, low-gradient continental shelf (De Santis and Caldara, 2016; De Santis et al., 2020a; De Santis et al., 2020b) with an abundant supply of sediment, and associated with dissipative beaches where constructional waves move sand onshore and alongshore resulting in beach accretion. These, as described by Fitzgerald et al. (2007), are the perfect conditions for the formation of a deltaic strandplain.

Progradation of the Carapelle deltaic strandplain occurred through the addition of beach ridges or cheniers. Beach ridges, which consist of wave-generated sand ridges, are a product of wave swash processes and may be topped by a thin deposit of aeolian sediment (Hesp et al., 2005; Fitzgerald et al., 2007). Cheniers are a special type of ridge. They are composed chiefly of sand and shell and are separated from adjacent ridges by mud or marshy deposits. Their formation has been related to the periodic deposition of fine and then coarser-grained sediment along the coast (Augustinus, 1989). Some of the relict ridges observed in the Carapelle deltaic strandplain may be also relict dune ridges, which can be present in a strandplain (Fitzgerald et al., 2007). Dune ridges in a strandplain have a greater elevation than beach ridges or cheniers and are essentially foredunes that become displaced from the beach due to shoreline progradation and new foredune construction.

The current low elevation of the linear features of the ancient Carapelle deltaic strandplain should exclude an aeolian origin, but we have to take into account that this characteristic can be the result of human flattening of coastal dunes in the study area (De Santis et al., 2023).

The data in our possession allow us to make a tentative reconstruction of the evolution of the Carapelle deltaic strandplain and the parallel history of AL2 and AL3 in Roman times (Figure 10).

With the analyses carried out to date on the trunks, we are unable to establish how far from the mouth the *Populus* trees originated, and therefore how far they were transported before being deposited where they were found, which is on the seaward side of at least three relict ridges that can be reconstructed from the aerial photographs (Figure 4). In any case, we believe that the most probable circumstance is that AL2 and AL3, before being uprooted and transported to the seaward side of the dunes or beach ridges, were germinated and grew somewhere in the deltaic strandplain or, at least, along the course of the Carapelle Stream.

There are, therefore, seven distinct steps of the evolutionary history of the Carapelle deltaic strandplain and AL2 and AL3.

- 1) Between 450 cal BC and 166 cal BC–8 cal AD: First step of development of the Carapelle deltaic strandplain. This step can be inferred from the interpretation of aerial photographs and stratigraphic data.
- 2) 166 cal BC–8 cal AD: birth of AL3. Since it is a *Populus*, we believe that AL3 was most probably born very close to the course of the Carapelle stream (Figure 10A).
- 3) 3–85 cal AD: birth of AL2. AL2 probably grew closer to the sea than AL3. Again, since it is a *Populus*, we believe that it grew very close to the course of the Carapelle Stream (Figure 10B).
- 4) 1–125 cal AD: death and subsequent transport of AL3 onto the beach, likely during an alluvial event. It was later moved northwards by littoral drift (and in this context colonised by barnacles) and then covered by beach sand, the context in which it was found (Figure 10C).
- 5) Between 1 and 125 cal AD and 246–383 cal AD: strong deltaic strandplain progradation and isolation of lagoons and/or ponds (Figure 10D).
- 6) 246–383 cal AD: death of AL2 and its transport into the lagoon/pond, likely during an alluvial event (Figure 10D).
- 7) Between 246 and 383 cal AD and 420–610 cal AD: Colonisation of AL2 by *Barnea candida* and burial in lagoon clays with *Cerastoderma glaucum*, the context in which AL2 was found (Figure 10E).

In our reconstruction, the modern counterpart most similar to the Roman-era Carapelle deltaic strandplain is represented by the current mouth of the Bevano Stream, which flows into the northern Adriatic (Figure 10F).

Overall, two main phases can be recognised in the evolution of the Carapelle deltaic strandplain:

- 1) a first phase of a continuous deltaic strandplain construction, lasted until ca. the birth of Christ, was characterised by a regular and continuous construction of sand ridges, one leaning against the other (see previous points 1, 2, and 3);

- 2) a second phase of discontinuous deltaic strandplain construction, lasted more or less from the birth of Christ to the termination of the construction of the deltaic strandplain, characterised by the construction of sand ridges/coastal barriers with the isolation of lagoons/ponds (see previous points 4, 5, and 6) and by evidences of alluvial events, testified by the death of the *Populus* trees and their transport onto the beach or lagoon. In addition, there is evidence, in the nearby Cervaro Stream (Figure 3), of the occurrence of alluvial events: specifically, an overbank episode was dated to 2140 ± 40 cal γ BP (190 ± 40 cal AD) (Caldara et al., 2022). Considering the proximity of the Cervaro Stream to the Carapelle Stream, it is extremely likely that the same event also affected the Carapelle Stream, and that other similar events affected the area in the same period.

The results provided by archaeological research contextualise the scenario in which the Carapelle deltaic strandplain developed in the Roman period.

The analysis of the archaeological material suggests the presence of anthropic traces over a long period (150 cal BC–800 cal AD), which partially corresponds to the formation of the Carapelle deltaic strandplain. In particular, the negligible presence of a single find referring to the period of 150–1 cal BC (a rim of Lamboglia 2) and the greater attested presence of late Roman ceramics dated to the period 390–700 cal AD supports the reconstructed chronology of the deltaic strandplain formation. The depth of the samples and the good state of preservation of the finds would support the hypothesis that the material could be representative of an archaeological deposit and could not have been affected by post-depositional processes. If confirmed, this scenario could give us more information on the path of the coastal Roman road that is cited by ancient sources (Polybius, 3.88.3; Livio, 9.2.6; Itinerarium Antoninum, 310.5) and described by scholars of ancient topography (Alvisi, 1970; Luisi, 1991; Volpe, 2002; Ceraudo, 2015; Marchi, 2019). It is likely that the road, which was called “Litoranea,” could have passed through here in the last phase of the deltaic strandplain formation, i.e., from about 390 cal AD, when the shoreline configuration was likely to have ensured the accessibility, viability and stability of the road. In the same way, the presence of a road here in earlier centuries can be ruled out. Such an interpretative hypothesis, developed from the integrated analysis of various sources (geomorphological, archaeological, historical, etc.) would fit into the broad context of studies on the evaluation of the ancient road system, partly confirming what is known (the potential presence of a coastal road in this area) and partly adding new elements to reconstruct the paleo-landscape (the potential route of a coastal Roman road in the last phase of the formation of the Carapelle deltaic strandplain).

5.2 Reconstruction of a possible climatic context during the Roman phase of Carapelle deltaic strandplain construction

According to many authors, the so-called Roman warm period (RWP) was the warmest period in Europe during the Holocene (Lamb, 1977; McCormick et al., 2012; Grauel et al., 2013; Hu et al., 2022), but it may have been a regional warming event limited to Europe and the North Atlantic. The warmest part (ca. 250–420 cal

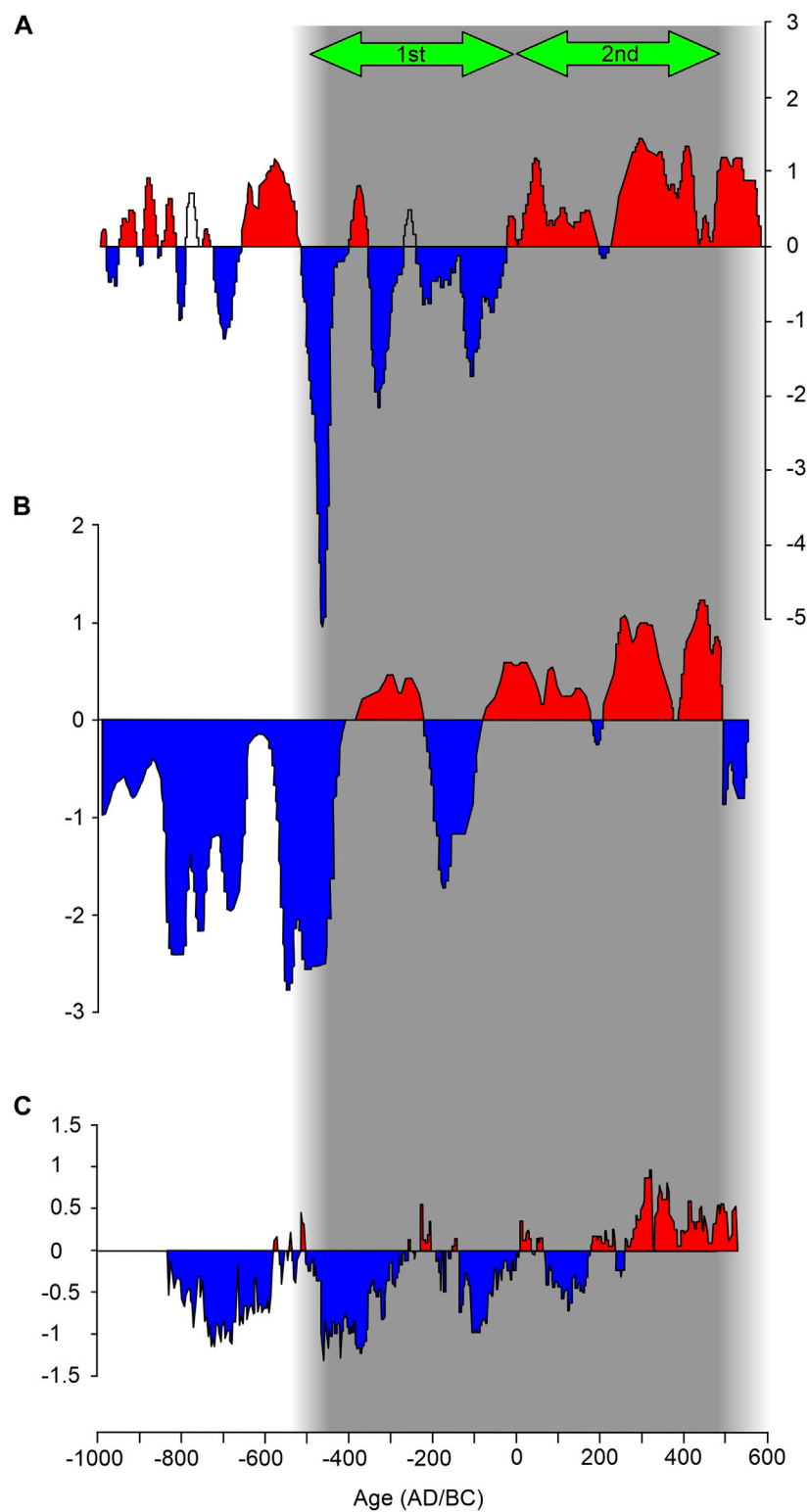


FIGURE 11

NAO index reconstructed by: (A) Baker et al. (2015), (B) Olsen et al. (2012), and (C) Faust et al. (2016). The grey band covers the period of formation of the Carapelle deltaic strandplain; the green arrows indicate the first and second phase of formation of the deltaic strandplain. Note that the first phase of the deltaic strandplain coincides with an overall negative NAO index, while the second phase coincides with an overall positive NAO index.

AD) of the RWP almost coincides with a warm phase in the northern hemisphere (Ljungqvist, 2010), suggesting a teleconnection between marine and continental systems.

Unfortunately, there is no formal agreement on the time interval covered by RWP (Grauel et al., 2013), so the boundaries are not precisely defined. In general, the widest time interval encompassing all the possible intervals proposed by different authors for RWP is ca. 550 cal BC to 450 cal AD (Grauel et al., 2013 and references therein).

Although the temperature reconstructions are quite coherent for RWP, all indicating general warming, it is not the same for the pattern of precipitation.

A sea surface temperature (SST) reconstruction from the Taranto Gulf (Apulia region, southern Italy), relatively close to the study site shows a first period lasting from 450 to 0 BC with relatively wet and warm conditions, followed by a second period (0–200 AD) characterised by more saline and oligotrophic water, and higher local terrestrial influences, which indicate drier conditions coupled with intensified deforestation within the Roman period (Grauel et al., 2013).

Recently, stalagmite-based climate records from 550 ± 10 cal BC to 950 ± 7 cal AD from northern Italy reveal a climatic trend of warming and increased humidity throughout the RWP (Hu et al., 2022).

Reconstruction of summer precipitation and temperature variability shows that wet and warm summers occurred during the Roman period in central Europe (Büntgen et al., 2011).

However, Magny et al. (2011, 2012) and Peyron et al. (2013) focused on the opposite hydrological pattern between northern-central and southern Mediterranean sites for the whole Holocene. Northern sites show warmer, drier conditions during the early to mid-Holocene, whereas cooler wetter conditions prevailed in southern Italy for the same period. This pattern is reversed in the late Holocene (between 5000 and 4000 cal. yr BP) with warmer drier conditions at southern sites and cooler wetter conditions at northern sites.

This assumption for the late Holocene in general is reinforced for the Roman period in particular if we take into account also the reconstructed North Atlantic Oscillation (NAO) index (Olsen et al., 2012; Baker et al., 2015) which suggests that the NAO shifted from a negative to a positive state during the RWP (Faust et al., 2016).

In fact, during a positive phase of the NAO, increased pressure contrasts between the Azores High and the Icelandic Low resulted in poleward migration of the westerlies over the North Atlantic, and increased precipitation in northern Europe. On the contrary, during a negative phase of the NAO, decreased pressure contrasts between the Azores High and the Icelandic Low resulted in southward migration of the westerlies and increased precipitation in southern Europe and the Mediterranean region (Hurrell and Deser, 2009).

Thus, a shift from negative to positive NAO index values during the RWP would suggest a shift of North Atlantic-driven precipitation towards the northern part of Italy and central-northern Europe, as indicated in the abovementioned works by Büntgen et al. (2011) and Hu et al. (2022). This resulted in an RWP that should have been characterised by a relatively dry phase in the southern Mediterranean area and, as a consequence, in the study

area. This pattern is confirmed by vegetation patterns (Di Rita and Magri, 2012; Di Rita et al., 2018; Margaritelli et al., 2020) with more open vegetation in the central Mediterranean area during the Roman period.

By comparing the Carapelle deltaic strandplain construction (with the first and second phase) with the NAO index reconstructions (Figure 11), we can see that the passage between the first and second phase of the Carapelle deltaic strandplain coincides with the passage from an overall negative NAO index to an overall positive NAO index. Thus, we argue that:

- 1) the first phase was triggered by a higher total amount of precipitations, but with less extreme alluvial events. This pattern resulted in a regular and continuous progradation of the deltaic strandplain by the continual addition of new sand ridges alongside the previous ones;
- 2) the second phase of the evolution was triggered by a total amount of precipitation lower than the previous period, but with higher occurrence of extreme alluvial events and/or by extreme alluvial events separated by longer period of low precipitations. This pattern resulted in a discontinuous construction of sand ridges/barriers and the isolation of lagoons/ponds. In particular, this higher occurrence of extreme alluvial events could have been promoted by:
 - a) the high SST in the Mediterranean during the RWP, which could have increased the temperature contrast between SST and the cold air from the N, NW and NE in autumn and winter. This could have induced more cyclogenesis and rain in the Mediterranean during autumn and winter, despite the onset of a positive phase of the NAO.
 - b) the ongoing vegetation opening—both climate- and human-induced—in the central Mediterranean during the Roman period (Di Rita and Magri, 2012), which could have accelerated soil erosion and, consequently, increased the sediment load and turbidity of rivers and streams.

Regarding changing vegetation in the central Mediterranean during the Roman period, pollen reconstructions from the Italian Peninsula have found only limited evidence of deforestation during the imperial period (Mensing et al., 2015 and references therein) but the whole Roman period shows evidence of more open vegetation and increasing human pressure on the natural landscape, as highlighted by many regional studies.

The analysis of fossil pollen in the sediments of Greece contemporary to the Roman Period (1st century BC to 5th century AD) reveals a continuous change from the pollen of Pine, *Rosaceae* and *Oleaceae* trees, which are typical of the so-called Mediterranean Forest, towards steppe pollen (Van Overloop, 1986; Reale and Dirmeyer, 2000).

On the French Mediterranean coast, the founding of Roman colonies is marked by the appearance of walnut pollen. Later deforestation is indicated by the decrease in forest tree pollen and an increase in the pollen of cultivated plants (Planchais, 1984; Hugues, 2011).

In the Gargano area, at the Lake Battaglia site (Caldara et al., 2008), a sharp collapse of the arboreal pollen (AP) concentrations

has been recorded at a depth of 4.20 m. The forest decline is associated with an increased frequency of fire. After the arboreal pollen drop, until around 2781 to 2665 cal yr BP (831–715 cal BC), mesophilous species were replaced by thermophilous taxa. The dominance of Chenopodiaceae, Gramineae and Cichorioideae suggests that a drier and warmer climate was established in coastal areas, and the Battaglia area was under an intensive regime of agropastoral exploitation (Caroli, 2005; Caroli and Caldara, 2007).

Very high resolution, annually resolved time series of anthropogenic deforestation in Europe over the past three millennia shows that—first in Greece (roughly 1000 cal BC to 300 cal BC) and several centuries later in Italy (roughly 300 cal BC to 200 cal AD)—the Classical Greek and Roman civilizations left their mark on the landscape, characterised by extensive forest clearance in these regions during these periods (Kaplan et al., 2009). Central and Western European deforestation is calculated to have been between 10% and 60%, while Eastern Europe, with lower population densities, remained highly forested. Williams (2000) provides recorded descriptions of extensive deforestation in these regions by the Greek author Homer (9th century BC) and the Roman author Lucretius (1st century BC), thus qualitatively verifying the model results of Kaplan et al. (2009). By AD 350, the collapse of the classical empires had led to lower population densities and reforestation in these areas relative to 300 BC.

Coastal pollen records in the central Mediterranean region show that the uppermost part of most sequences, including the Roman period, are characterised by a transition to open or semi-open landscapes, with the expansion of several herbaceous taxa (Di Rita and Magri, 2012).

In the Rieti basin in central Italy, forests declined during the Imperial period compared to the Republican period. The total AP changed from 81% to 66% (Mensing et al., 2015). According to Favre et al. (2008), an AP percentage of over 70%–80% is considered to represent a forested environment that has not been impacted by humans, whereas values below 40%–50% indicate open environments that have been strongly impacted by humans through deforestation. Intermediate percentages (as in the Rieti basin) are indicative of a patchy landscape with forested areas and open spaces, pointing to a moderate to weak impact of humans on the forest cover.

In the Sant'Eufemia plain, AP percentages showed a sharp decrease, from between 50% and 75% in the Greek period to between 20% and 30% in the Roman period. Although this decrease could have been partly driven by natural factors, it is coupled with a pronounced increase in microcharcoal, suggesting that fires represented a common practice for clearing forests, creating open spaces for agricultural and pastoral activities, and producing charcoal (Russo Ermolli et al., 2018).

To conclude, the most probable climatic–environmental scenario that promoted the formation of the Roman deltaic strandplain by the Carapelle Stream includes reduced total precipitation relative to the previous period, but with extreme events causing floods and high sediment load, which was enhanced by vegetation opening. The interpretation of the Carapelle deltaic strandplain as a first continuous and then discontinuous strandplain reinforces the scenario, in which the progradation occurred in a first phase in a continuous mode and in a second phase mostly following discrete

alluvial events, that isolated ponds or small lagoons between the sand ridges of the strandplain.

6 Conclusion

In this work, we document the construction of a deltaic strandplain during the Roman period at the mouth of the Carapelle stream, in the coastal sector of the Tavoliere di Puglia, the second largest Italian plain. The construction of this coastal system is a remarkable geomorphological imprint of the Roman warm period; it was interrupted at the end of the Roman period and has never been repeated in more recent times up to the present, neither by the Carapelle stream, nor by other streams that cross the Tavoliere di Puglia. Through a multidisciplinary study we have reconstructed a scenario in which two main factors could have contributed to the construction of this landform: an increase in the frequency of extreme flood events and an opening of the vegetation, the latter probably caused by both climatic factors and human activity. The construction of the deltaic strandplain most likely premised the creation of a Roman coastal road during the imperial age.

The three tree trunks coeval with the construction phase of this landform, exhumed fortuitously, will be the basis for further research; in fact, in the future we expect to analyze in depth the growth rings of these trunks to better define the climatic context we have reconstructed.

Data availability statement

The original contributions presented in the study are included in the article/[Supplementary Material](#), further inquiries can be directed to the corresponding author.

Ethics statement

Written informed consent was obtained from the individual(s) for the publication of any identifiable images or data included in this article.

Author contributions

VD: Conceptualization, Data curation, Formal Analysis, Investigation, Methodology, Software, Supervision, Validation, Visualization, Writing—original draft, Writing—review and editing. GSi: Formal Analysis, Funding acquisition, Investigation, Methodology, Project administration, Resources, Supervision, Validation, Writing—review and editing. GSa: Data curation, Investigation, Writing—review and editing. DM: Data curation, Investigation, Methodology, Writing—review and editing. RS: Data curation, Investigation, Methodology, Writing—review and editing. GC: Methodology, Resources, Writing—review and editing, Data curation, Investigation. MZ: Data curation, Investigation, Methodology, Writing—review and editing. NA: Data curation, Investigation, Methodology, Writing—review and editing. VT: Data curation, Investigation, Methodology, Writing—review and editing. MC: Data curation, Formal Analysis,

Funding acquisition, Investigation, Methodology, Project administration, Resources, Supervision, Validation, Writing—review and editing.

Funding

The authors declare financial support was received for the research, authorship, and/or publication of this article. This research was partially funded by the Research Agreement stipulated between the University of Bari Aldo Moro and the Agenzia Regionale Strategica per lo Sviluppo Ecosostenibile del Territorio (ASSET, Italy) for the development of the STREAM project (“Strategic Development of Flood Management” CUP J99E20000370001, Scientific Coordinator GSi); Progetto di Rilevante Interesse Nazionale (PRIN) GAIA Prot. 2022ZSMRXJ—Geomorphological and hydrogeological vulnerability of Italian coastal areas in response to sea level rise and marine extreme events. Coordinator: Prof. Mastronuzzi Giuseppe Antonio.

Acknowledgments

We are very grateful to farmland owners for the permission to access and make boreholes. We also are grateful to Department of

Soil, Plant and Food Sciences of University of Bari “Aldo Moro” for the use of instruments and tools for studying of trunks.

Conflict of interest

The authors declare that the research was conducted in the absence of any commercial or financial relationships that could be construed as a potential conflict of interest.

Publisher’s note

All claims expressed in this article are solely those of the authors and do not necessarily represent those of their affiliated organizations, or those of the publisher, the editors and the reviewers. Any product that may be evaluated in this article, or claim that may be made by its manufacturer, is not guaranteed or endorsed by the publisher.

Supplementary material

The Supplementary Material for this article can be found online at: <https://www.frontiersin.org/articles/10.3389/feart.2023.1278105/full#supplementary-material>

References

- Áilc, U. (2010). Synanthropic vegetation: pattern of various disturbances on life history traits. *Acta Bot. Croat.* 69 (2). Available at: <https://www.abc.botanic.hr/index.php/abc/article/view/318>.
- Allen, J. R. M., Watts, W. A., McGee, E., and Huntley, B. (2002). Holocene environmental variability—The record from lago grande di Monticchio, Italy. *Quat. Int.* 88, 69–80. doi:10.1016/S1040-6182(01)00074-X
- Alvisi, G. (1970). La viabilità romana della Daunia. Società Storia Patria Bari Available at: <https://www.unilibro.it/libro/alvisi-giovanna/la-viabilita-romana-della-daunia/892358> (Accessed July 12, 2023).
- Amorosi, A., Bruno, L., Caldara, M., Campo, B., Cau, S., De Santis, V., et al. (2023). Late quaternary sedimentary record of estuarine incised-valley filling and interfluvial flooding: the Manfredonia paleovalley system (southern Italy). *Mar. Petroleum Geol.* 147, 105975. doi:10.1016/j.marpetgeo.2022.105975
- Andronico, D., and Cioni, R. (2002). Contrasting styles of Mount Vesuvius activity in the period between the Avellino and Pompeii Plinian eruptions, and some implications for assessment of future hazards. *Bull. Volcanol.* 64, 372–391. doi:10.1007/s00445-002-0215-4
- Angiolini, C., de Simone, L., Fiaschi, T., Cifaldi, G. P., Maccherini, S., and Fanfarillo, E. (2023). Detecting the imprints of past clear-cutting on riparian forest plant communities along a Mediterranean river. *River Res. Appl.* doi:10.1002/rra.4152
- Arnò, V., Principe, C., Rosi, M., Santacroce, R., Sbrana, A., and Sheridan, M. F. (1987). “Eruptive history,” *Somma Vesuvius*. Editor R. Santacroce (CNR Quaderni Ricerca Sci), 114, 53–103.
- Augustinus, P. G. E. F. (1989). Cheniers and chenier plains: a general introduction. *Mar. Geol.* 90, 219–229. doi:10.1016/0025-3227(89)90126-6
- Baker, A., Hellstrom, J., Kelly, B. F. J., Mariethoz, G., and Trouet, V. (2015). A composite annual-resolution stalagmite record of North Atlantic climate over the last three millennia. *Sci. Rep.* 5, 10307. doi:10.1038/srep10307
- Bar-Matthews, M., and Ayalon, A. (2011). Mid-Holocene climate variations revealed by high-resolution speleothem records from Soreq Cave, Israel and their correlation with cultural changes. *Holocene* 21, 163–171. doi:10.1177/0959683610384165
- Bianchi, C. N. (1981). Guide per il riconoscimento delle specie animali delle acque lagunari e costiere italiane (5). Available at: <https://www.unilibro.it/libro/bianchi-c-n/guide-riconoscimento-specie-animale-acque-lagunari-costiere-italiane-5-/867357> (Accessed July 12, 2023).
- Boenzi, F., Caldara, M., Moresi, M., and Pennetta, L. (2001). History of the salpi lagoon-sabha (Manfredonia Gulf, Italy). *Alp. Mediterr. Quat.* 14 (2), 93–104.
- Boenzi, F., Caldara, M., and Pennetta, L. (1992). *Osservazioni stratigrafiche e geomorfologiche del tratto meridionale della piana costiera del Tavoliere di Puglia*. Geografia Fisica e Dinamica Quaternaria, 23–31.
- Boenzi, F., Caldara, M., Pennetta, L., and Simone, O. (2006). Environmental aspects related to the physical evolution of some wetlands along the adriatic coast of Apulia (southern Italy): a review. *J. Coast. Res.*, 170–175.
- Bojnanský, V., and Fargašová, A. (2007). *Atlas of seeds and fruits of central and east-European flora: the carpathian Mountains region*. 2007th edition. Springer.
- Bond, G., Kromer, B., Beer, J., Muscheler, R., Evans, M. N., Showers, W., et al. (2001). Persistent solar influence on North Atlantic climate during the Holocene. *Science* 294, 2130–2136. doi:10.1126/science.1065680
- Bond, G., Showers, W., Cheseby, M., Lotti, R., Almasi, P., deMenocal, P., et al. (1997). A pervasive millennial-scale cycle in North Atlantic Holocene and glacial climates. *Science* 278, 1257–1266. doi:10.1126/science.278.5341.1257
- Bonifay, M. (2004). *Etudes sur La ceramique romaine tardive d’Afrique*. Oxford, England: BAR Publishing.
- Bonifay, M. (2007). “Que transportaient donc les amphores africaines?,” in *Supplying Rome and the empire. The proceedings of an international seminar held at siena-certosa di Pontignano an may 2-4, 2004 on Rome, the provinces, production and distribution, JRA, suppl. Ser. 69, portsmouth*. Editor E. Papi (Rhode Island), 8–31.
- Bradley, R. S., Hughes, M. K., and Diaz, H. F. (2003). Climate in medieval time. *Science* 302, 404–405. doi:10.1126/science.1090372
- Brayshaw, D. J., Hoskins, B., and Black, E. (2010). Some physical drivers of changes in the winter storm tracks over the North Atlantic and Mediterranean during the Holocene. *Philosophical Trans. Math. Phys. Eng. Sci.* 368, 5185–5223. doi:10.1098/rsta.2010.0180
- Bronk Ramsey (2021). *OxCal v.4.4.4*.
- Bruno, S., Galdo, G. G. D., Guarino, R., and Minissale, P. (2007). A survey of the weedy communities of sicily. *Ann. Bot.* 7. doi:10.4462/annbotrm-9091
- Bruno, S., and Guarino, R. (2007). The mediterranean weedy vegetation and its origin. *Ann. Bot.* 7. doi:10.4462/annbotrm-9089
- Bruno, B., and Bocchio, S. (2005). *Le anfore da trasporto*. La ceramica ei materiali di età romana, 353–394.
- Büntgen, U., Tegel, W., Nicolussi, K., McCormick, M., Frank, D., Trouet, V., et al. (2011). 2500 Years of European climate variability and human susceptibility. *Science* 331, 578–582. doi:10.1126/science.1197175

- Cacciari, M., Amorosi, A., Marchesini, M., Kaniewski, D., Bruno, L., Campo, B., et al. (2020). Linking Holocene vegetation dynamics, palaeoclimate variability and depositional patterns in coastal successions: insights from the Po Delta plain of northern Italy. *Palaeogeogr. Palaeoclimatol. Palaeoecol.* 538, 109468–109469. doi:10.1016/j.palaeo.2019.109468
- Caggiani, M. C., Ditaranto, N., Guascito, M. R., Acquafredda, P., Laviano, R., Giannossa, L. C., et al. (2015). Combined analysis of enamelled and gilded glassware from Frederick II castle at Melfi (Italy) to identify technology and raw materials: SEM-EDS, Raman, LA-ICPMS, XPS analysis of enamelled and gilded glass. *X-Ray Spectrom* 44, 191–200. doi:10.1002/xrs.2594
- Caldara, M., Capolongo, D., Del Gaudio, V., De Santis, V., Pennetta, L., and Maiorano, P. (2022). *Note Illustrative Della Carta Geologica d'Italia alla Scala 1: 50.000 Foglio, 409 "Zapponeta."* Istituto Superiore per la Protezione e la Ricerca Ambientale: roma. Italy. Available at: https://www.isprambiente.gov.it/Media/carg/note_illustrative/409_Zapponeta.pdf.
- Caldara, M., Caroli, I., and Simone, O. (2008). Holocene evolution and sea-level changes in the Battaglia basin area (eastern Gargano coast, Apulia, Italy). *Quat. Int.* 183, 102–114. doi:10.1016/j.quaint.2007.07.005
- Caldara, M., and Pennetta, L. (1992). Interpretazione paleoclimatica di dati preistorici e storici relativi all'entroterra del Golfo di Manfredonia. *Mem. DELLA SOCIETA' Geol. Ital.* 42 (1989), 197–207.
- Caldara, M., Pennetta, L., and Simone, O. (2002). Holocene evolution of the salpi lagoon (Puglia, Italy). *J. Coast. Res.* 36, 124–133. doi:10.2112/1551-5036-36.sp1.124
- Caroli, I., and Caldara, M. (2007). Vegetation history of lago Battaglia (eastern Gargano coast, Apulia, Italy) during the middle-late Holocene. *Veg. Hist. Archaeobotany* 16, 317–327. doi:10.1007/s00334-006-0045-y
- Caroli, I. (2005). "Dinamiche climatiche ed ambientali dell'area garganica nel corso dell'Olocene." Ph.D. Thesis, Università degli Studi di Bari, in *Facoltà di Scienze Matematiche, Fisiche e Naturali, Dipartimento di Geologia e Geofisica*.
- Cattaneo, A., Correggiari, A., Langone, L., and Trincardi, F. (2003). The late-holocene Gargano subaqueous delta, adriatic shelf: sediment pathways and supply fluctuations. *Mar. Geol.* 193, 61–91. doi:10.1016/S0025-3227(02)00614-X
- Ceci, M., and Valenzani, R. S. (2016). "Analisi, quantificazione e interpretazione," in *La ceramica nello scavo archeologico* (Roma: Carocci).
- Ceraudo, G. (2015). "La via Appia (a sud di Benevento) e il sistema stradale in Puglia tra Pirro e Annibale," in *Atti 52° convegno di Studi sulla magna grecia*, 211–245. Taranto 2012, Napoli 2014, Available at: https://www.academia.edu/16478425/La_Via_Appia_a_sud_di_Benevento_e_il_sistema_stradale_in_Puglia_tra_Pirro_e_Annibale_in_Atti_52_Convegno_di_Studi_sulla_Magna_Grecia_Taranto_2012_Napoli_2014_pp_211_245 (Accessed July 12, 2023).
- Correggiari, A., Trincardi, F., Langone, L., and Roveri, M. (2001). Styles of failure in late Holocene highstand prodelta wedges on the adriatic shelf. *J. Sediment. Res.* 71, 218–236. doi:10.1306/042800710218
- Dall'Aglio, P. L. (2000). Il terreno e le sue rappresentazioni: il survey e la ricerca storico-topografica. *Topogr. Antica. Manuali Sci.*, 1000–1009. doi:10.1400/86357
- De Mitri, C. D. (1993). "La ceramica romana e tardo antica," in *Il complesso tardo-antico ed alto-medievale dei SS. Cosma e Damiano, detto "Le Centoporte", Giurdignano (LE). Scavi 1993–1996*. Editors P. ARTHUR and B. BRUNO, 137–150. Available at: https://www.academia.edu/1629755/10_La_ceramica_romana_e_tardo_antica_in_P_ARTHUR_BRUNO_B_eds_il_complesso_tardo_antico_ed_alto_medievale_dei_SS_Cosma_e_Damiano_detto_Le_Centoporte_Giurdignano_LE_Scavi_1993_1996_pp_137_150 (Accessed August 4, 2023).
- De Santis, V., Caldara, M., de Torres, T., and Ortiz, J. E. (2010). Stratigraphic units of the apulian Tavoliere plain (southern Italy): chronology, correlation with marine isotope stages and implications regarding vertical movements. *Sediment. Geol.* 228, 255–270. doi:10.1016/j.sedgeo.2010.05.001
- De Santis, V., and Caldara, M. (2016). Evolution of an incised valley system in the southern Adriatic Sea (apulian margin): an onshore-offshore correlation. *Geol. J.* 51, 263–284. doi:10.1002/gj.2628
- De Santis, V., Caldara, M., Marsico, A., Capolongo, D., and Pennetta, L. (2018). Evolution of the ofanto river delta from the 'little ice age' to modern times: implications of large-scale synoptic patterns. *Holocene* 28, 1948–1967. doi:10.1177/0959683618798109
- De Santis, V., Caldara, M., and Pennetta, L. (2014). The marine and alluvial terraces of Tavoliere di Puglia plain (southern Italy). *J. Maps* 10, 114–125. doi:10.1080/17445647.2013.861366
- De Santis, V., Caldara, M., Pennetta, L., Torres, T., and Ortiz, J. E. (2013). Unconformity-bounded stratigraphic units (UBSUs) in an Italian alluvial plain area: recognizing and dating. *J. Sediment. Res.* 83, 96–113. doi:10.2110/jsr.2013.7
- De Santis, V., Caldara, M., and Pennetta, L. (2020b). Transgressive architecture of coastal barrier systems in the ofanto incised valley and its surrounding shelf in response to stepped sea-level rise. *Geosciences* 10, 497. doi:10.3390/geosciences10120497
- De Santis, V., Caldara, M., and Pennetta, L. (2020a). "Continuous" backstepping of Holocene coastal barrier systems into incised valleys: insights from the ofanto and carapelle-cervaro valleys. *Water* 12, 1799. doi:10.3390/w12061799
- De Santis, V., and Caldara, M. (2015). The 5.5–4.5 kyr climatic transition as recorded by the sedimentation pattern of coastal deposits of the Apulia region, southern Italy. *Holocene* 25, 1313–1329. doi:10.1177/0959683615584207
- De Santis, V., Caldara, M., Torres, T., Ortiz, J. E., and Sánchez-Palencia, Y. (2020c). The role of beach ridges, spits, or barriers in understanding marine terraces processes on loose or semiconsolidated substrates: insights from the givoni of the Gulf of Taranto (southern Italy). *Geol. J.* 55, 2951–2975. doi:10.1002/gj.3550
- De Santis, V., Rizzo, A., Scardino, G., Scicchitano, G., and Caldara, M. (2023a). A procedure for evaluating historical land use change and resilience in highly reclaimed coastal areas: the case of the Tavoliere di Puglia (southern Italy). *Land* 12, 775. doi:10.3390/land12040775
- Di Geronimo, I. (1984). Stabilité des peuplements benthiques et stabilité des bassins sédimentaires. *Geobios* 17, 145–150. doi:10.1016/S0016-6995(84)80167-9
- Di Rita, F., Fletcher, W. J., Aranbarri, J., Margaritelli, G., Lirer, F., and Magri, D. (2018). Holocene forest dynamics in central and western mediterranean: periodicity, spatio-temporal patterns and climate influence. *Sci. Rep.* 8, 8929. doi:10.1038/s41598-018-27056-2
- Di Rita, F., and Magri, D. (2012). An overview of the Holocene vegetation history from the central Mediterranean coasts. *J. Mediterr. Earth Sci.* 4, 35–52. doi:10.3304/JMES.2012.003
- Di Rita, F., Simone, O., Caldara, M., Gehrels, W. R., and Magri, D. (2011). Holocene environmental changes in the coastal Tavoliere plain (Apulia, southern Italy): a multiproxy approach. *Palaeogeogr. Palaeoclimatol. Palaeoecol.* 310, 139–151. doi:10.1016/j.palaeo.2011.06.012
- Dibenedetto, G. (1988). "Le bonifiche in Capitanata nella prima metà del XIX secolo." in *Atti 6° Convegno Preistoria, Protostoria e Storia della Daunia* (San Severo), 95–120.
- Disantarosa, G. (2015). "Le anfore e gli opercula," in *Archeologia urbana a Bari nell'area della Basilica di San Nicola, saggi 1982-1984-1987*. Editors M. R. Depalo, G. Disantarosa, and D. Nuzzo (Bari), 175–201.
- Disantarosa, G. (2010). "Le anfore vinarie attestate nelle Puglie. A. Calò, L. Bertoldi Lenoci, Storia regionale della vite e del vino," in *Le puglie (Daunia, Terra di Bari, Terra d'Otranto)* (Martina Franca), 81–144.
- Disantarosa, G. (2007). Vecchi recuperi subacquei a Bari e nuove interpretazioni. *L'Archeologo subacqueo* XIII (1), 6–8.
- Dogliani, C., Mongelli, F., and Pieri, P. (1994). The Puglia uplift (SE Italy): an anomaly in the foreland of the apenninic subduction due to buckling of a thick continental lithosphere. *Tectonics* 13, 1309–1321. doi:10.1029/94TC01501
- Dogliani, C., Tropeano, M., Mongelli, F., and Pieri, P. (1996). Middle-late Pleistocene uplift of Puglia: an "anomaly" in the apenninic foreland. *Mem. Soc. Geol. Ital.* 51, 101–117. doi:10.1029/94TC01501
- Fanelli, G., and Lucchese, F. (1998). Lo status delle comunità dei Brometalia rubentictorum del Mediterraneo in differenti schemi sintattonomici. *Rend. Fis. Acc. Lincei* 9, 241–255. doi:10.1007/BF02904407
- Faust, J. C., Fabian, K., Milzer, G., Giraudeau, J., and Knies, J. (2016). Norwegian fjord sediments reveal NAO related winter temperature and precipitation changes of the past 2800 years. *Earth Planet. Sci. Lett.* 435, 84–93. doi:10.1016/j.epsl.2015.12.003
- Favre, E., Escarguel, G., Suc, J.-P., Vidal, G., and Thévenod, L. (2008). A contribution to deciphering the meaning of AP/NAP with respect to vegetation cover. *Rev. Palaeobot. Palynology* 148, 13–35. doi:10.1016/j.revpalbo.2007.08.003
- Ferrari, K. (2017). Studying evolving landscapes: geomorphology as a research tool for landscape archaeology. *Theor. Roman Archaeol. J.* 115, 115. doi:10.16995/TRAC2016_115_132
- FitzGerald, D., Cleary, W., Buynevich, I., Hein, C., Klein, A. H., Asp, N., et al. (2007). Strandplain evolution along the southern coast of Santa Catarina, Brazil. *J. Coast. Res.* 152–156.
- Gafta, D. (1993). Zonation et dynamisme de la végétation dans quelques forêts rivariennes de l'Italie du sud. *Coll. Phytosoc.* 20, 233–240.
- Giaime, M., Artzy, M., Jol, H. M., Salmon, Y., López, G. I., and Abu Hamid, A. (2022). Refining Late-Holocene environmental changes of the Akko coastal plain and its impacts on the settlement and anchorage patterns of Tel Akko (Israel). *Mar. Geol.* 447, 106778. doi:10.1016/j.margeo.2022.106778
- Grauel, A.-L., Goudeau, M.-L., de Lange, G., and Bernasconi, S. (2013). Climate of the past 2500 years in the Gulf of Taranto, central mediterranean sea: a high-resolution climate reconstruction based on $\delta^{18}O$ and $\delta^{13}C$ of globigerinoides ruber (white). *Holocene* 23, 1440–1446. doi:10.1177/0959683613493937
- Hesp, P. A., Dillenburg, S. R., Barboza, E. G., Tomazelli, L. J., Ayup-Zouain, R. N., Esteves, L. S., et al. (2005). Beach ridges, foredunes or transgressive dunefields? Definitions and an examination of the torres to tramandaí barrier system, southern Brazil. *An. Acad. Bras. Ciênc.* 77, 493–508. doi:10.1590/S0001-37652005000300010
- Hu, H.-M., Michel, V., Valensi, P., Mii, H.-S., Starnini, E., Zunino, M., et al. (2022). Stalagmite-inferred climate in the western mediterranean during the roman Warm Period. *Climate* 10, 93. doi:10.3390/cli10070093
- Hughes, J. D. (2011). Ancient deforestation revisited. *J. Hist. Biol.* 44, 43–57. doi:10.1007/s10739-010-9247-3
- Hurrell, J. W., and Deser, C. (2009). North atlantic climate variability: the role of the North atlantic oscillation. *J. Mar. Syst.* 78, 28–41. doi:10.1016/j.jmarsys.2008.11.026

- Isaia, R., D'Antonio, M., Dell'Erba, F., Di Vito, M. A., and Orsi, G. (2004). The Astroni volcano: the only example of closely spaced eruptions in the same vent area during the recent history of the campi flegrei caldera (Italy). *J. Volcanol. Geotherm. Res.* 133, 171–192. doi:10.1016/S0377-0273(03)00397-4
- Isla, M. F., Moyano-Paz, D., FitzGerald, D. M., Simontacchi, L., and Veiga, G. D. (2023). Contrasting beach-ridge systems in different types of coastal settings. *Earth Surf. Process. Landforms* 48 (1), 47–71. doi:10.1002/esp.5429
- Kaplan, J. O., Krumhardt, K. M., and Zimmermann, N. (2009). The prehistoric and preindustrial deforestation of Europe. *Quat. Sci. Rev.* 28, 3016–3034. doi:10.1016/j.quascirev.2009.09.028
- Karymbalis, E., Tsanakas, K., Cundy, A., Iliopoulos, G., Papadopoulou, P., Protopappas, D., et al. (2022). Late Holocene palaeogeographic evolution of the lihoura coastal plain, pteleos Gulf, Central Greece. *Quat. Int.* 638–639, 70–83. doi:10.1016/j.quaint.2021.12.007
- Lamb, H. H. (1977). Climate: present, past and future. Available at: <https://www.booktopia.com.au/climate-present-past-and-future-hubert-lamb/book/9780415682237.html> (Accessed July 12, 2023).
- Ljungqvist, F. C. (2010). A new reconstruction of temperature variability in the extra-tropical northern hemisphere during the last two millennia. *Geogr. Ann. Ser. A, Phys. Geogr.* 92, 339–351. doi:10.1111/j.1468-0459.2010.00399.x
- López-Belzunce, M., Blázquez, A. M., Carmona, P., and Ruiz, J. (2020). Multi proxy analysis for reconstructing the late Holocene evolution of a mediterranean coastal lagoon: environmental variables within foraminiferal assemblages. *Catena* 187, 104333. doi:10.1016/j.catena.2019.104333
- Luisi, A. (1991). “La viabilità nell'Apulia antica,” in *Idea e realtà del viaggio. Il viaggio nel mondo antico*. Editors G. Camassa and S. Fasce (Genova: Nuova Atlantide), 261–269.
- Magny, M., Peyron, O., Sadori, L., Ortu, E., Zanchetta, G., Vannière, B., et al. (2012). Contrasting patterns of precipitation seasonality during the Holocene in the south- and north-central Mediterranean. *J. Quat. Sci.* 27, 290–296. doi:10.1002/jqs.1543
- Magny, M., Vannière, B., Calo, C., Millet, L., Leroux, A., Peyron, O., et al. (2011). Holocene hydrological changes in south-western Mediterranean as recorded by lake-level fluctuations at Lago Preola, a coastal lake in southern Sicily, Italy. *Quat. Sci. Rev.* 30, 2459–2475. doi:10.1016/j.quascirev.2011.05.018
- Marchi, M. L. (2019). “Dalla terra al mare: i percorsi e le dinamiche insediative fra entroterra e costa adriatica nella Puglia settentrionale fra IV e III secolo a.C.,” in *I paesaggi costieri dell'Adriatico tra Antichità e Altomedioevo*. Editors C. S. Fiorello and F. Tassaux, 135–148. Available at: https://www.academia.edu/39944833/Dalla_terra_al_mare_i_percorsi_e_le_dinamiche_insediative_fra_entroterra_e_costa_adriatica_nella_Puglia_settentrionale_fra_IV_e_III_secolo_a_C_in_C_S_Fiorello_F_Tassaux_I_paesaggi_costieri_dell_Adriatico_tra_Antichità_e_Altomedioevo_Bordeaux_2019_pp_135_148 (Accessed July 12, 2023).
- Margaritelli, G., Cacho, I., Català, A., Barra, M., Bellucci, L. G., Lubritto, C., et al. (2020). Persistent warm Mediterranean surface waters during the Roman period. *Sci. Rep.* 10, 10431. doi:10.1038/s41598-020-67281-2
- Maselli, V., and Trincardi, F. (2013). Large-scale single incised valley from a small catchment basin on the western Adriatic margin (central Mediterranean Sea). *Glob. Planet. Change* 100, 245–262. doi:10.1016/j.gloplacha.2012.10.008
- Mayewski, P. A., Rohling, E. E., Curt Stager, J., Karlén, W., Maasch, K. A., David Meeker, L., et al. (2004). Holocene climate variability. *Quat. Res.* 62, 243–255. doi:10.1016/j.yqres.2004.07.001
- McCormick, M., Büntgen, U., Cane, M. A., Cook, E. R., Harper, K., Huybers, P., et al. (2012). Climate change during and after the roman empire: reconstructing the past from scientific and historical evidence. *J. Interdiscip. Hist.* 43, 169–220. doi:10.1162/jinh_a_00379
- McCubbin, D. G. (1982). *Barrier-island and strand-plain facies*, 247–279.
- Mele, D., Costa, A., Dellino, P., Sulpizio, R., Dioguardi, F., Isaia, R., et al. (2020). Total grain size distribution of components of fallout deposits and implications for magma fragmentation mechanisms: examples from campi flegrei caldera (Italy). *Bull. Volcanol.* 82, 31. doi:10.1007/s00445-020-1368-8
- Melis, R. T., Di Rita, F., French, C., Marriner, N., Montis, F., Serreli, G., et al. (2018). 8000 years of coastal changes on a western mediterranean island: a multiproxy approach from the posada plain of sardinia. *Mar. Geol.* 403, 93–108. doi:10.1016/j.margeo.2018.05.004
- Mensing, S. A., Tunno, I., Sagnotti, L., Florindo, F., Noble, P., Archer, C., et al. (2015). 2700 years of mediterranean environmental change in central Italy: a synthesis of sedimentary and cultural records to interpret past impacts of climate on society. *Quat. Sci. Rev.* 116, 72–94. doi:10.1016/j.quascirev.2015.03.022
- Moy, C. M., Seltzer, G. O., Rodbell, D. T., and Anderson, D. M. (2002). Variability of El Niño/southern oscillation activity at millennial timescales during the Holocene epoch. *Nature* 420, 162–165. doi:10.1038/nature01194
- Mucina, L., Bültmann, H., Dierßen, K., Theurillat, J.-P., Raus, T., Čami, A., et al. (2016). Vegetation of Europe: hierarchical floristic classification system of vascular plant, bryophyte, lichen, and algal communities. *Appl. Veg. Sci.* 19, 3–264. doi:10.1111/avsc.12257
- O'Brien, S. R., Mayewski, P. A., Meeker, L. D., Meese, D. A., Twickler, M. S., and Whitlow, S. I. (1995). Complexity of Holocene climate as reconstructed from a Greenland ice core. *Science* 270, 1962–1964. doi:10.1126/science.270.5244.1962
- Occhipinti Ambrogi, A. (1981). Guide per il riconoscimento delle specie animali delle acque lagunari e costiere italiane (7). Available at: <https://www.unilibro.it/libro/occhipinti-ambrogi-a/-guide-riconoscimento-specie-animale-acque-lagunari-costiere-italiane-7/867359> (Accessed August 4, 2023).
- Olsen, J., Anderson, N. J., and Knudsen, M. F. (2012). Variability of the North atlantic oscillation over the past 5,200 years. *Nat. Geosci.* 5, 808–812. doi:10.1038/ngeo1589
- Otvos, E. G. (2000). Beach ridges — Definitions and significance. *Geomorphology* 32, 83–108. doi:10.1016/S0169-555X(99)00075-6
- Otvos, E. G. (2022). Coastal barrier morphogenic categories in Mississippi Delta plain development. *Mar. Geol.* 454, 106931. doi:10.1016/j.margeo.2022.106931
- Panella, C. (1998). Archeologia subacquea, come opera l'archeologo sott'acqua. Available at: <https://maredicarta.com/libreria/archeologia-subacquea-come-opera-l-archeologo-sott-acqua/t/160565> (Accessed August 4, 2023).
- Panella, C. (2001). Le anfore di età imperiale del Mediterraneo occidentale. *Collect. de l'Institut des Sci. Tech. de l'Antiquité* 720, 177–276.
- Péres, J.-M., Picard, J., and Picard, J. (1964). *Nouveau manuel de bionomie benthique de la mer Méditerranéenne*. Station Marine d'Endoume.
- Péres, J.-M. (1967). The Mediterranean benthos. *Oceanogr. Mar. Biol. Annu. Rev.* Available at: <http://www.vliz.be/en/imis?refid=79714> (Accessed February 9, 2021).
- Peyron, O., Magny, M., Goring, S., Joannin, S., de Beaulieu, J.-L., Brugiapaglia, E., et al. (2013). Contrasting patterns of climatic changes during the Holocene across the Italian Peninsula reconstructed from pollen data. *Clim. Past* 9, 1233–1252. doi:10.5194/cp-9-1233-2013
- Piéri, D. (2005). *Le commerce du vin oriental à l'époque byzantine (Ve-VIIe siècles): le témoignage des amphores en gaule. Illustrated edizione*. Beyrouth: Institut français d'archéologie du Proche-Orient.
- Planchais, N. (1984). Palynologie lagunaire: l'exemple du Languedoc-roussillon. *Ann. Géogr.* 93, 268–275.
- Reale, O., and Dirmeyer, P. (2000). Modeling the effects of vegetation on mediterranean climate during the roman classical period: part I: climate history and model sensitivity. *Glob. Planet. Change* 25, 163–184. doi:10.1016/S0921-8181(00)00002-3
- Reimer, P. J., Austin, W. E. N., Bard, E., Bayliss, A., Blackwell, P. G., Ramsey, C. B., et al. (2020). The IntCal20 northern hemisphere radiocarbon age calibration curve (0–55 cal kBP). *Radiocarbon* 62, 725–757. doi:10.1017/RDC.2020.41
- Renfrew, C., and Bahn, P. (2016). *Archaeology: theories, methods, and practice*. Seventh edition. London: Thames & Hudson.
- Riccato, A. (2020). AQUILEIA. FONDI COSSAR 3.2. La ceramica da cucina: produzioni italice e orientali. *Scavi Aquil. II*. Available at: https://www.academia.edu/44394465/AQUILEIA_FONDI_COSSAR_3_2_La_ceramica_da_cucina_produzioni_italiche_e_orientali (Accessed August 4, 2023).
- Ricchetti, G., Ciaranfi, N., Luperto Sinni, E., Mongelli, F., and Pieri, P. (1992). Geodinamica ed evoluzione sedimentaria e tettonica dell'avampaese apulo. *Mem. della Soc. Geol. Ital.* 41, 57–82.
- Rivas-Martínez, S., Díaz, T., Fernández-González, F., Izco, J., Loidi, J., Lousã, M., et al. (2002). Vascular plants communities of Spain and Portugal. Addenda to the syntaxonomical checklist of 2001. *Part II. Itinera Geobot.* 15, 433–922.
- Roberts, N., Brayshaw, D., Kuzucuoglu, C., Perez, R., and Sadori, L. (2011). The mid-holocene climatic transition in the mediterranean: causes and consequences. *Holocene* 21, 3–13. doi:10.1177/0959683610388058
- Rolandi, G., Petrosino, P., and Mc Geehin, J. (1998). The interplinian activity at Somma-Vesuvius in the last 3500 years. *J. Volcanol. Geotherm. Res.* 82, 19–52. doi:10.1016/S0377-0273(97)00056-5
- Russo Ermolli, E., Ruello, M. R., Cicala, L., Di Lorenzo, H., Molisso, F., and Pacciarelli, M. (2018). An 8300-yr record of environmental and cultural changes in the Sant'Eufemia Plain (Calabria, Italy). *Quat. Int.* 483, 39–56. doi:10.1016/j.quaint.2018.01.033
- Sacchi, M., Molisso, F., Pacifico, A., Vigliotti, M., Sabbarese, C., and Ruberti, D. (2014). Late-holocene to recent evolution of lake patria, south Italy: an example of a coastal lagoon within a mediterranean delta system. *Glob. Planet. Change* 117, 9–27. doi:10.1016/J.GLOPLACHA.2014.03.004
- Santacroce, R., Cioni, R., Marianelli, P., Sbrana, A., Sulpizio, R., Zanchetta, G., et al. (2008). Age and whole rock-glass compositions of proximal pyroclastics from the major explosive eruptions of somma-vesuvius: a review as a tool for distal tephrostratigraphy. *J. Volcanol. Geotherm. Res.* 177, 1–18. doi:10.1016/j.jvolgeores.2008.06.009
- Schmiedt, G. (1973). Contributo della fotografia aerea alla ricostruzione della antica laguna compresa fra Siponto e Salapia. *Arch. Stor. Pugliese* 26, 159–172.
- Sevink, J., van Bergen, M. J., van der Plicht, J., Feiken, H., Anastasia, C., and Huizinga, A. (2011). Robust date for the bronze age Avellino eruption (Somma-Vesuvius): 3945 ± 10 calBP (1995 ± 10 calBC). *Quat. Sci. Rev.* 30, 1035–1046. doi:10.1016/j.quascirev.2011.02.001
- Shepard, F. P., Phleger, F. B., and Andel, T. H. V. (1960). Recent sediments, northwest Gulf of Mexico. *Am. Assoc. Petroleum Geol.* doi:10.1306/SV21353
- Sinopoli, C. M. (1991). *Approaches to archaeological ceramics*. 1991st edition. New York: Springer.

- Smith, V. C., Isaia, R., and Pearce, N. J. G. (2011). Tephrostratigraphy and glass compositions of post-15 kyr campi flegrei eruptions: implications for eruption history and chronostratigraphic markers. *Quat. Sci. Rev.* 30, 3638–3660. doi:10.1016/j.quascirev.2011.07.012
- Stuiver, M., and Reimer, P. J. (1993). Extended 14C data base and revised CALIB 3.0 14C age calibration program. *Radiocarbon* 35, 215–230. doi:10.1017/S0033822200013904
- Sulpizio, R., Cioni, R., Di Vito, M. A., Mele, D., Bonasia, R., and Dellino, P. (2010). The Pomice di Avellino eruption of somma-vesuvius (3.9 ka BP). Part I: stratigraphy, compositional variability and eruptive dynamics. *Bull. Volcanol.* 72, 539–558. doi:10.1007/s00445-009-0339-x
- Susini, D., Vignola, C., Goffredo, R., Totten, D. M., Masi, A., Smedile, A., et al. (2023). Holocene palaeoenvironmental and human settlement evolution in the southern margin of the Salpi lagoon, Tavoliere coastal plain (Apulia, Southern Italy). *Quat. Int.* 655, 37–54. doi:10.1016/j.quaint.2022.10.012
- Tomaselli, V., Beccarisi, L., Cambria, S., Forte, L., Minissale, P., Sciandrello, S., et al. (2022). Validation of associations for the temporary ponds of the class Isoeto-Nanojuncetea in Puglia (southern Italy). *Mediterr. Bot.* 43, e80627. doi:10.5209/mbot.80627
- Tomaselli, V., Veronico, G., Sciandrello, S., and Forte, L. (2020). Therophytic halophilous vegetation classification in South-Eastern Italy. *Phytocoenologia* 50, 187–209. doi:10.1127/phyto/2020/0364
- Totten, D. M. (2022). “Late Roman Painted and Unpainted Common Ware (Ceramica comune dipinta e acroma): 4th-8th c. CE at Salapia,” in *Salapia-Salpi I. Scavi e ricerche 2013-2016*. Editors G. De Venuto, R. Goffredo, and D. M. Totten (Bari, 329–370).
- Trincardi, F., Cattaneo, A., Alessandra, A., Correggiari, A., and Langone, L. (1996). Stratigraphy of the late-Quaternary deposits in the Central Adriatic basin and the record of short-term climatic events. *Memorie-Istituto Ital. Di Idrobiol.* 55, 39–70.
- Van Overloop, E. (1986). “Comparison of climatic evolution during post-glacial times in Greece, tropical and subtropical regions,” in *Relation to desertification. In desertification in Europe*. Editors R. Fantechi and N. S. Margaris (Dordrecht: Springer Netherlands), 59–72. doi:10.1007/978-94-009-4648-4_6
- Vatova, A. (1949). La fauna bentonica dell’Alto e Medio Adriatico. *Nova Thalass.* 1–100.
- Volpe, G. (2002). “Viabilità e insediamenti nell’Apulia romana,” in *Territorio e identità regionali. La storia della Puglia* (Edipuglia), 57–66.
- Wanner, H., Solomina, O., Grosjean, M., Ritz, S. P., and Jetel, M. (2011). Structure and origin of Holocene cold events. *Quat. Sci. Rev.* 30, 3109–3123. doi:10.1016/j.quascirev.2011.07.010
- Williams, M. (2000). Dark ages and dark areas: global deforestation in the deep past. *J. Hist. Geogr.* 26, 28–46. doi:10.1006/jhge.1999.0189
- Zanchetta, G., Giraudi, C., Sulpizio, R., Magny, M., Drysdale, R. N., and Sadori, L. (2012). Constraining the onset of the Holocene “Neoglacial” over the central Italy using tephra layers. *Quat. Res.* 78, 236–247. doi:10.1016/j.yqres.2012.05.010
- Zingaro, M., La Salandra, M., Colacicco, R., Roseto, R., Petio, P., and Capolongo, D. (2021). Suitability assessment of global, continental and national digital elevation models for geomorphological analyses in Italy. *Trans. GIS* 25, 2283–2308. doi:10.1111/tgis.12845
- Zingaro, M., and Mastronuzzi, G. (2017). Il popolamento antico di Lama Diurno-San Giorgio in relazione alle forme del paesaggio. *Agri centuriati* 14, 39–56.